The θ–S relations in the northern seas: Implications for the deep circulation

BERT RUDELS

Rudels, B. 1986: The θ–S relations in the northern seas: Implications for the deep circulation. *Polar Research 4 n.s.*, 133–159.

The θ–S relations for the cold, saline deep and bottom waters in the Greenland and Norwegian Seas and the Polar Ocean are displayed and discussed. The differences in θ–S curves are explained by a mixing of the deep water masses and by the injection of waters from above consisting of cold dense water formed by cooling and ice formation at the sea surface and entrained warm water from the intermediate layers. Estimates of the strength of the deep water circulation are based upon the changes in θ–S curves and on some assumptions about the transformations of the Bering Strait inflow in the Chukchi Sea and on the Alaskan shelf.

Bert Rudels, Norwegian Polar Research Institute, N-1330 Oslo Lufthavn, Norway; October 1984 (revised May 1986).

1. Introduction

The main features of the water mass distribution in the northern seas – the Norwegian Sea, the Greenland Sea and the Polar Ocean – have been known since the turn of the century, when there was a spur of activity (Helland-Hansen & Koefoed 1907; Helland-Hansen & Nansen 1909; Mohn 1887; Nansen 1902, 1906). The hydrography and bathymetry of these seas are already well described in Coachman & Aagaard 1974, and we shall here give only a brief summary.

The water masses in all basins are dominated by the cold and almost isohaline deep and bottom waters. In the Norwegian Sea this water mass is covered by warm Atlantic water entering from the south and flowing north towards the Fram Strait. This Atlantic cover is also present, albeit somewhat colder, in the Polar Ocean, where it has become submerged by the cold, low, saline, polar surface water.

The situation is rather different in the Greenland Sea. Here the lighter upper layers are confined to the periphery, to the outflow of polar surface water and Atlantic water in the East Greenland Current to the west and to the northward drift of Atlantic water in the Norwegian Sea to the east. In the central Greenland Sea gyre the deep water is found close to the sea surface and not isolated from the atmosphere by a warm Atlantic layer.

This condition led Nansen to the conclusion that the Greenland Sea gyre was a centre of extensive deep water formation, which then replenished the other basins. The differences, which exist in temperatures and salinities between the different basins, seem to support such a view. The Greenland Sea deep water (GSDW) is the coldest ($-1.28 < \theta < -1.0$) and least saline ($S \sim 34.89$), the minimum temperature and salinity gradually increasing to $\theta \sim -1.07$ and $S \sim 34.91$ in the Norwegian Sea and $\theta \sim -0.97$°C and $S \sim 34.94$ in the Polar Ocean (Swift et al. 1983).

However, a closer look at the temperature and salinity distributions makes the view that these changes can come about only through turbulent diffusive heating from above rather unlikely. Especially the question of the origin of the Polar Ocean deep water (PODW) has been reopened lately (Swift et al. 1983; Aagaard et al. 1985). Does it derive solely from the Greenland/Norwegian Seas or are, in addition, processes inside the Polar Ocean actively contributing to the PODW and changing its θ–S characteristics from the relatively cold, fresh signature of the GSDW to the warmer, more saline values found inside the polar basin?

The question is not new, and the situation is quite similar to the one which Nansen faced, with even higher odds, after the results obtained from the 'Fram' expedition (Nansen 1902). The high salinities ($S \sim 35.15\%$ and now known to be erroneous) then observed in the PODW obliged him to search for another possible, more saline source, which in addition to the presumed inflow from the Greenland/Norwegian Seas through the Fram Strait could account for the observed values. In fact, half of Nansen's monograph, Northern Waters, is devoted to this problem, and his attention is directed towards the eastern Barents Sea as a possible source. Excessive ice formation over the shallow banks close to Novaja Zemlja may produce cold, saline and dense water. He also presented observations, which showed saline ($S > 35$ ‰) bottom water with temperatures at the freezing point in the eastern deep depressions of the Barent Sea. However, no continuous flow of such water from the Barents Sea into the Polar Ocean could be found neither through Franz Victoria Renna nor through the St. Anna Trough. With the salinities observed from 'Veslemøy' north of Svalbard (Nansen 1915), Nansen then decided that the salinities measured onboard 'Fram' were too high, and embraced the view that the PODW derived, through the Fram Strait, from the deep water formation area in the Greenland Sea.

In the subsequent work Nansen's conjecture was accepted, and the attention was focused on the nature of the deep water formation process (Carmack & Aagaard 1973; Kiilerich 1945; Killworth 1979; McDougall 1983; Metcalf 1955; Mosby 1959, 1961), but rarely was the exchange of deep water through the Fram Strait discussed. This can to a large extent be explained by the lack of good hydrographic data from the Polar Ocean and to an inferior knowledge of the bathymetry

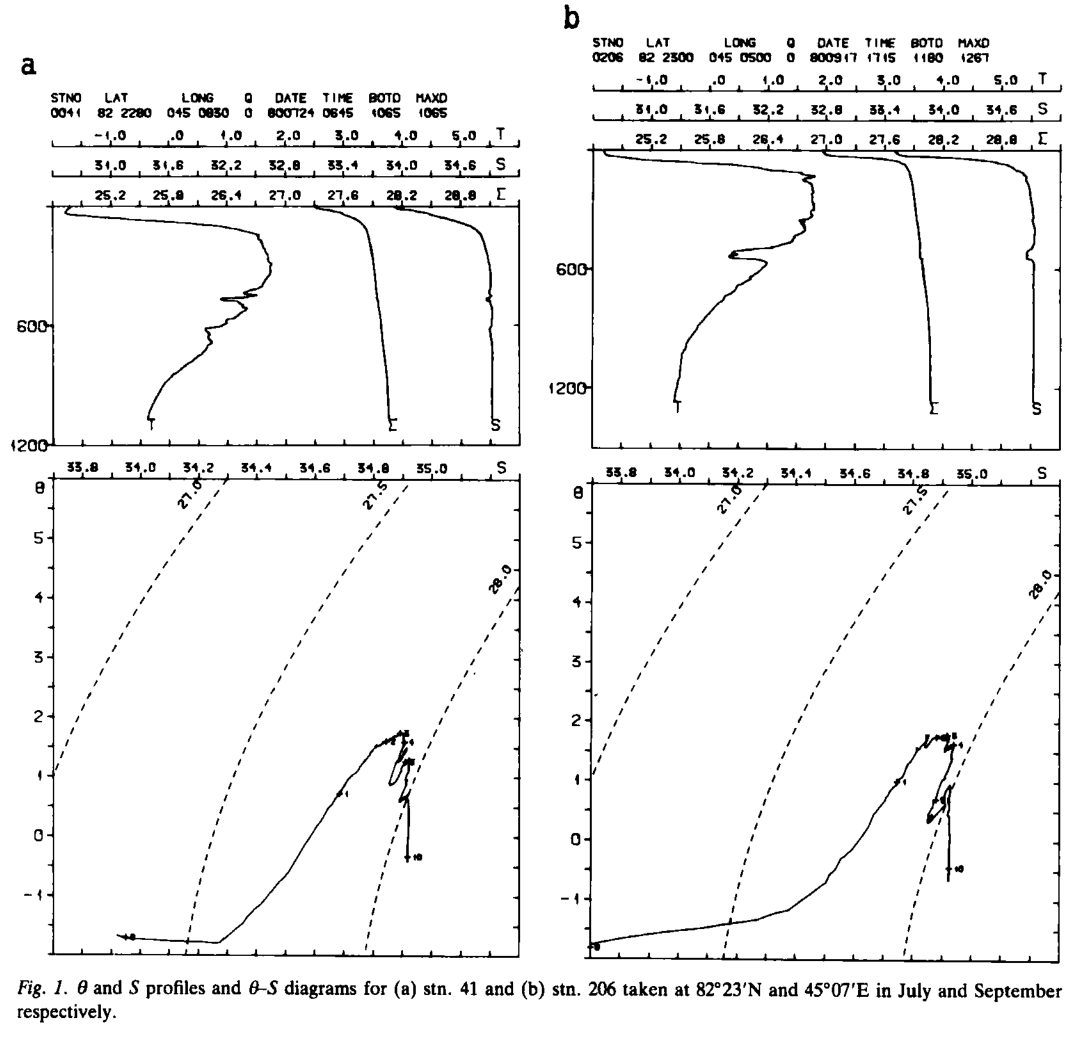

Fig. 1. θ and S profiles and θ–S diagrams for (a) stn. 41 and (b) stn. 206 taken at 82°23′N and 45°07′E in July and September respectively.

of the Fram Strait. However, the warmer, more saline nature of the deep Polar Ocean as compared to the Greenland Sea was recognized. One suggested explanation for this feature was that due to some unidentified dynamical constraint only Norwegian Sea deep water (NSDW) and not GSDW entered the polar basin (Metcalf 1960; Palfrey 1967).

Still, this is not enough to explain the higher temperatures and salinities encountered in the deep Polar Ocean. This fact became more and more obvious with the improvement of the measuring techniques, and with the paper by Swift et al. (1983) we were suddenly back pondering over the same question as Nansen 80 years ago, albeit with lower salinities ($S \sim 34.94\%$) in the PODW to explain. Meanwhile, many others of Nansen's conjectures were vindicated. Shallow shelf areas are regions where saline water with temperature at freezing point is produced by ice formation and brine rejection. This has been seen not only in the eastern Barents Sea, but also in the area closer to Svalbard (Midttun 1985) and on the Alaskan shelf (Aagaard et al. 1981).

Inspection of θ–S diagrams has shown that the halocline found all over the Polar Ocean between the Atlantic layer and the upper homogeneous polar mixed layer cannot be the result of a direct mixing between these waters, it must have an advective origin (Coachman & Barnes 1962). Probable source areas for the halocline are the shelves, where brine rejection may create water with the required density and θ–S characteristics, and Aagaard et al. (1981) treated this problem in considerable detail. They assumed that the water discharging from the shelves was dense enough to form the halocline, but not to penetrate deeper into the water column. However, the high salinities found on some shelves (as mentioned above) indicate that such a deep sinking would be possible.

This is one of the few processes which could explain the salinities and temperatures observed in the deeper layers of the Polar Ocean, and Aagaard et al. (1985) have put forth such a view. So far no plume sinking from the shelves into the deep interior of the Polar Ocean has been observed, nor has the flow of cold dense water from the Barents Sea into the Polar Ocean, which Nansen was looking for, been found. This may be because these events occur but rarely, and are difficult to detect. A flow of water less dense than the deep water, but still dense enough to sink beneath the Atlantic layer may be inferred from the θ–S curves from some stations taken from HMS 'Ymer' in the northeastern Barents Sea and on the continental slope northwest of Franz Josef Land (Fig. 1). The notion that the temperature and salinity minimum found northwest of Franz Josef Land represents a plume, which leaves the Barents Sea and follows the slope towards the east, is strengthened by the two subsequent observations two months apart on the same location. The minimum found on station 206 also showed a high Cs-137 concentration indicating a recent sinking event (E. Holm pers. comm.). The minimum is absent further to the west (Fig. 2a) on the same isobath, and θ–S diagrams from stations taken in the northern Barents Sea (Fig. 2b) show that water in the indicated θ–S range is present in the passage between Franz Josef Land and Victoria Island and could supply the observed minimum.

In some sense the state of our knowledge of the processes determining the θ–S structure in the Polar Ocean resembles the one we have for the Greenland Sea. None of the inferred convection events have as yet been observed, and what we assume to happen is based upon conjectures and analogies with other areas (Carmack & Aagaard 1973; McDougall 1983; Killworth 1979, 1981; Clarke & Gascard 1983; Gascard & Clarke 1983).

2. The observation material and the inferred circulation

In the present section we shall simply display some θ–S curves from the colder denser layer ($\theta < 0$, $S > 34.80$) in the Greenland/Norwegian Seas and the Polar Ocean. The stations in the Polar Ocean and the Fram Strait were taken by HMS 'Ymer' in the summer of 1980, while the Greenland Sea observations were made from 'M/S Polarsirkel' in April 1980. Several deep stations taken in some 'crucial' areas have been plotted on the same diagram to enhance the visual 'feel' for the θ–S structure, its scatter and shape as well as the quality of the data. The values have been taken from data lists and plotted by hand. The salinities from the 'Polarsirkel' showed several large jumps during the cruise. Here these jumps have been removed by taking the salinity at 3000 m to be $S = 34.893 \pm 0.003$ for all stations. The station locations are shown in Fig. 3. We do

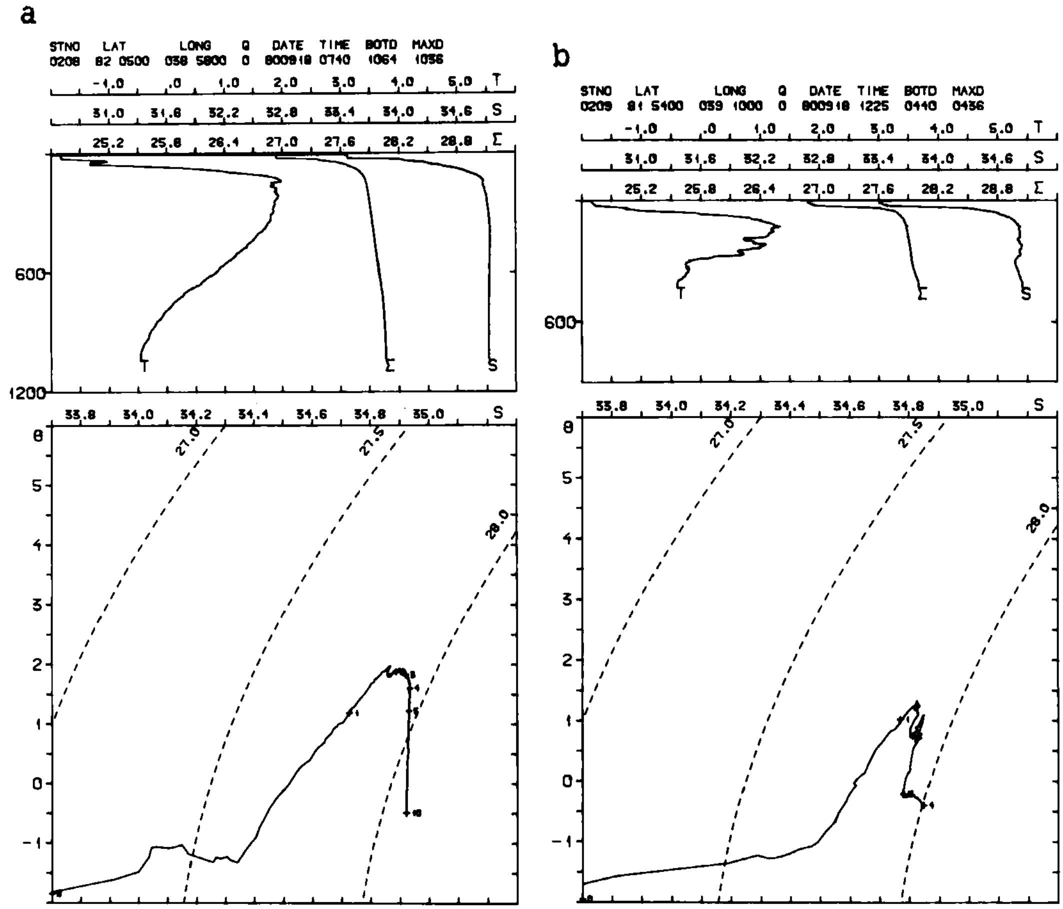

Fig. 2. θ and *S* profiles and θ–*S* diagrams for (a) stn. 208 82°05′N, 38°58′E, (b) stn. 209 81°54′N, 39°10′E.

not claim the same accuracy for these data as e.g. those presented by the PACODF group at Scripps Oceanographic Institute. Still, we do believe that maxima observed at an individual station are real. And the persistent presence of a maximum and a minimum in an area is taken as a sign that we are not observing an artifact of the instruments.

We shall try to follow the deep water on its assumed path between and inside the different seas, note the differences which exist in the θ–*S* curves, and, if possible, try to suggest processes which might be responsible for the observed changes. We will emphasize the differences between areas, how they affect the processes and the signals which we expect to observe.

Due to the shallow sills (600–850 m) to the south between Greenland and Scotland, the Polar Ocean and the Greenland/Norwegian Seas form an almost closed system with respect to the deep circulation. We shall therefore finally attempt to estimate how vigorous the circulation of the deep water between the different northern seas is, as compared to the southward export of deep water to the North Atlantic.

The θ–*S* diagrams of the water masses, which we shall discuss, are shown in Figs. 4, 6, 8. We may note that in some areas, notably the Greenland Sea gyre, the entire water column is found in the range $\theta < 0$, $S > 34.8$. More commonly though, the deep water is isolated from the atmosphere by a warm Atlantic layer ($\theta > 0$, $S > 34.90$) (Swift & Aagaard 1981) as in the Norwegian Sea, while in the Polar Ocean, the Fram Strait, and over the Greenland continental slope we have the additional cover of low saline polar water which was mentioned in the introduction above.

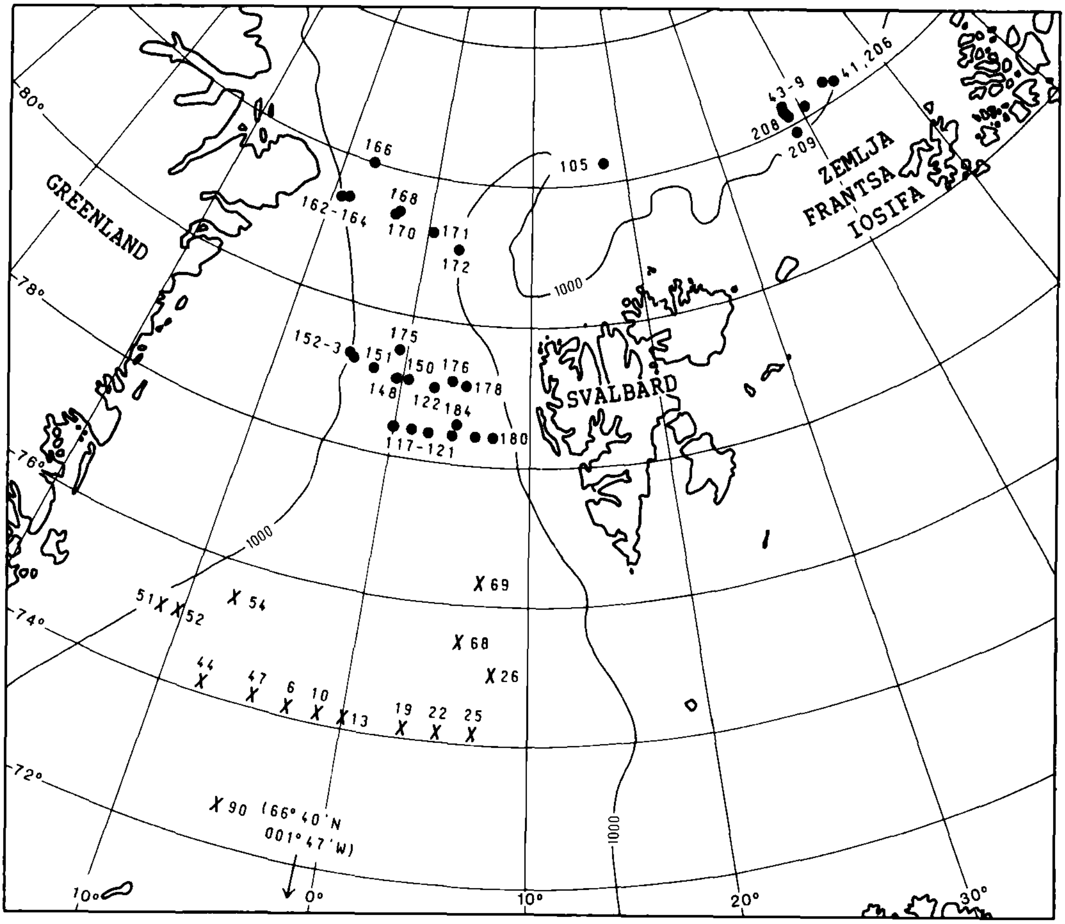

Fig. 3. Chart showing the positions of the stations used in this work. Dots denote 'Polarsirkel' and Crosses, 'Ymer' stations.

Between these principal water masses there are transition layers, most of which are water masses in their own right. The pycnocline found in the Polar Ocean is advected from the shelves (Aagaard et al. 1981), and the salinity minimum observed between 500 and 1000 m in the eastern Fram Strait is probably the result of a homogenization of the upper layers in the Greenland Sea (Swift & Aagaard 1981; Rudels & Anderson 1982; Aagaard et al. 1985).

The most coherent inflow into the Polar Ocean takes place west of Svalbard in the West Spitsbergen Current. This current carries mainly warm Atlantic water, but we may expect that it also transports water in the deeper layers. The deep water found over the Svalbard continental slope has a tight θ–S curve in the temperature range below zero (Figs. 4a, b) and closely resembles the θ–S curves found in the Norwegian Sea (Fig. 4c). This contrasts with the conditions further to the west in the deeper part of the Fram Strait, where a much broader θ–S relation and a generally fresher water column is found (Fig. 4d). The 'noisy' structure indicates interleaving of different water masses, and here we observe mixing between NSDW and fresher deep water from the Greenland Sea, as compared to the almost exclusive NSDW over the Svalbard slope.

Inside the Polar Ocean in the area north of Svalbard and Franz Josef Land (Fig. 4e) the situation is different, and two features deserve notice. 1. The deepest layers have higher salinity and temperature. The temperature is rather constant (−0.95°C) at depths below 2000 m, while the salinity shows an increase with depth towards the bottom. The high deep and bottom salinity will

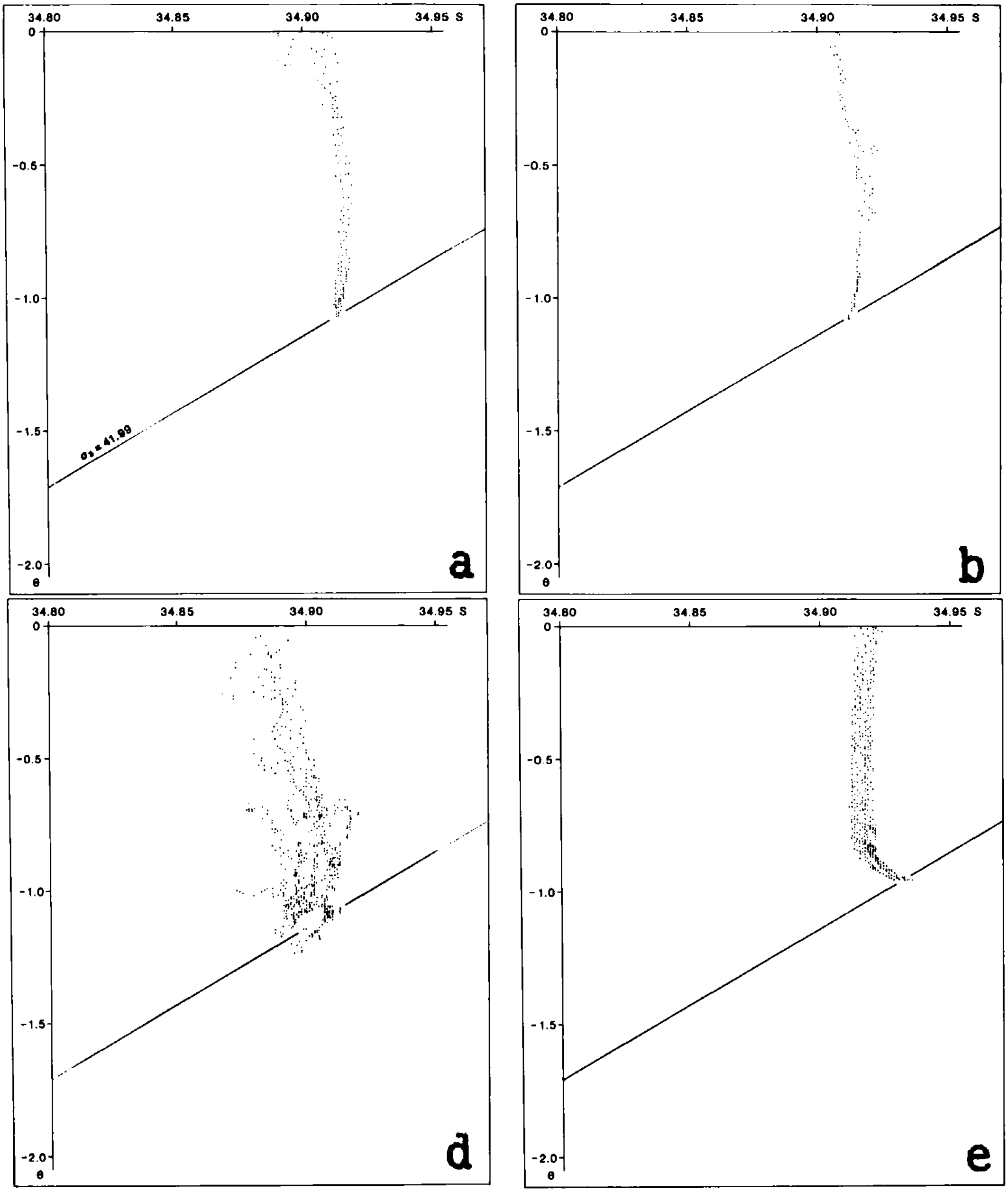

be discussed more fully in section 3.1. 2. In the upper deep layers we have again a tight θ–S relationship with an almost constant salinity of 34.92 in the temperature range $-0.9°\mathrm{C} < \theta < 0°\mathrm{C}$.

The constant salinity of $S \sim 34.92$ in the upper deep layers (Fig. 4e) suggests that these layers consist mainly of an inflow of NSDW through the Fram Strait and/or that most of the intrusions observed in the Fram Strait have been removed, presumably by double diffusive processes. There is a very weak salinity minimum around $\theta \sim -0.6$, which could be a remnant of intrusions of GSDW or other low saline waters. Another explanation might be that salt has been lost downwards from the Atlantic layer by salt fingering and accumu-

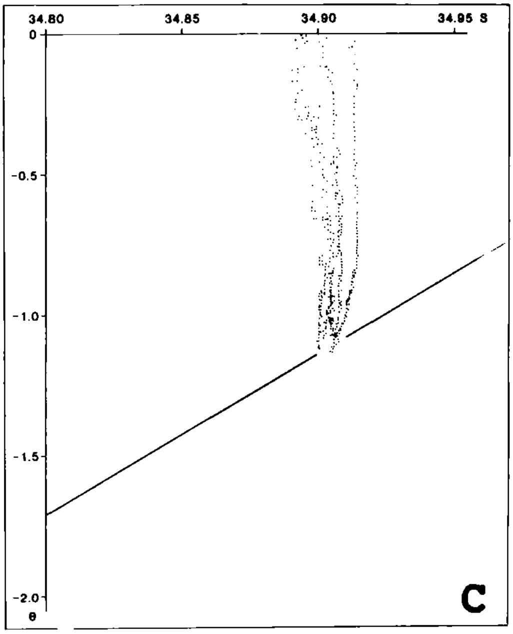

Fig. 4a. θ–S curves from stations taken on the western slope of Svalbard. Station numbers Y-180, Y-183, Y-184. *b.* θ–S curves from stations taken on the western slope of the Yermak plateau. Station numbers Y-171, Y-172. *c.* θ–S curves from stations taken in the Norwegian Sea and in the eastern part of the Greenland Sea, where Atlantic water is present in the upper layers. Station numbers P-25, P-26, P-68, P-69, P-90. *d.* θ–S curves from deep stations in the eastern part of the Fram Strait. Station numbers Y-117, Y-118, Y-119, Y-120, Y-121. *e.* θ–S curves from stations taken north-west of Franz Josef Land. Station numbers Y-43, Y-44, Y-45, Y-46, Y-47, Y-48, Y-49, Y-50.

lated at the temperature range $-0.5°C < \theta < 0°C$. This is possible close to the Fram Strait, where the Atlantic layer still constitutes a salinity maximum. The layer could also account for the increase in salinity below the temperature maximum which is observed when stations west and north of Svalbard are compared (Fig. 5).

It is also conceivable that the minimum at the Fram Strait stations, which was commented upon above, is trapped in the Fram Strait. Because of the presence of the Yermak plateau to the east it may not enter the Polar Ocean in any significant amount.

In the expected outflow region northeast of Greenland the θ–S curves have changed still further. The highly saline bottom water is still found (Fig. 6a), but the possible weak minimum at $\theta \sim -0.6°C$ has been replaced by another upper salinity maximum. By contrast the salinity around $\theta \sim 0°C$ has decreased.

The upper salinity maximum most likely results from the presence of deep water from the Canadian basin, which has passed over the Lomonosov ridge and leaves through the Fram Strait. The temperature of this deep water, about −0.5°C, is due to the Lomonosov ridge, which prevents the colder bottom water in the Eurasian basin from entering the Canadian basin (Coachman & Aagaard 1974). The salinity in the Canadian basin is high – $S \sim 34.95$ – compared to 34.92 for the same temperature range in the Eurasian basin (Aagaard 1981). See also Fig. 4d. The higher salinities in the Canadian basin show that processes which affect the deeper layers are present there too.

The lowering of the salinity in the upper layers poses a more difficult but perhaps a related problem. Is the decrease due to cold, less saline intrusions entering on that density level or to a loss of salt to the upper low saline surface layers?

As we move south into the Greenland Sea we encounter different regimes, whether we follow the continental slope or enter into the deeper part of that sea. The upper salinity maximum (at $\theta = -0.6°C$) appears to follow the slope while it slowly weakens (Fig. 6b). In the deeper parts of the basin this maximum is mostly absent, and the

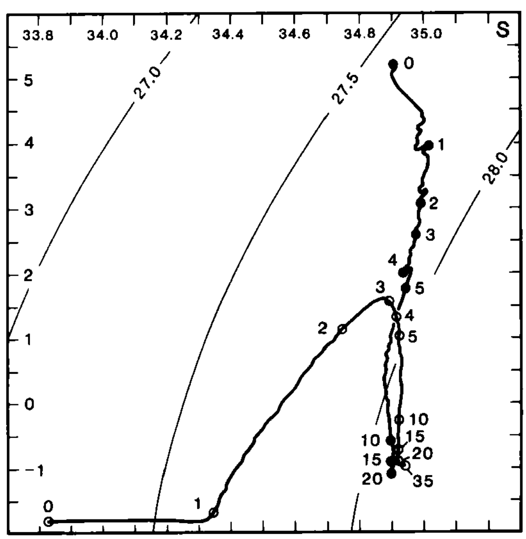

Fig. 5. θ–S curves from stn. Y-118 in the Fram Strait and stn. Y-105 north of Svalbard.

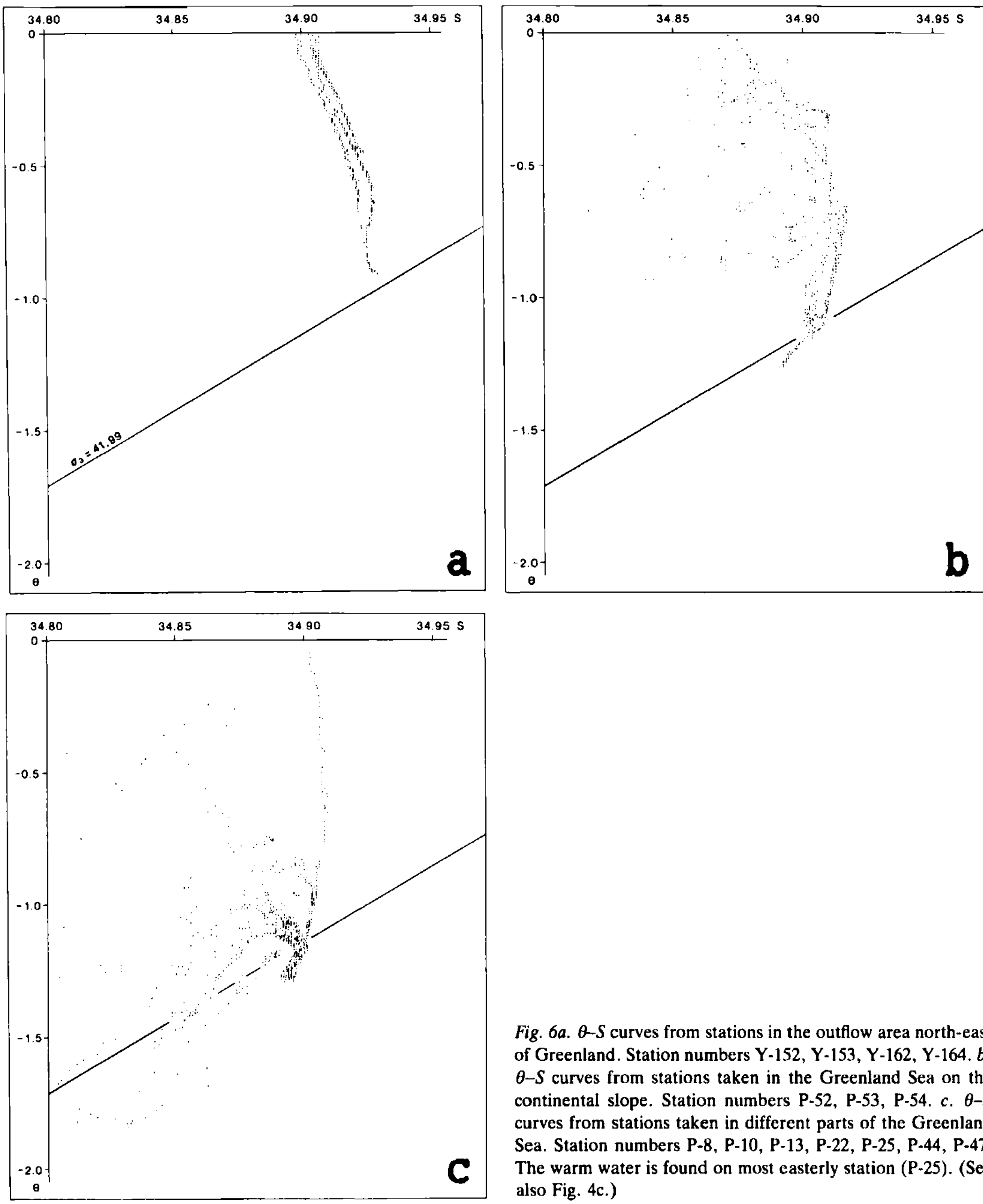

Fig. 6a. θ–S curves from stations in the outflow area north-east of Greenland. Station numbers Y-152, Y-153, Y-162, Y-164. *b.* θ–S curves from stations taken in the Greenland Sea on the continental slope. Station numbers P-52, P-53, P-54. *c.* θ–S curves from stations taken in different parts of the Greenland Sea. Station numbers P-8, P-10, P-13, P-22, P-25, P-44, P-47. The warm water is found on most easterly station (P-25). (See also Fig. 4c.)

water column is much colder and fresher (Fig. 6c). For the bottom water we notice a tendency towards colder, fresher values, which contrasts with the corresponding high salinities found in the Polar Ocean. We shall discuss these differences below.

The difference in θ–S characteristics between the slope and the deeper parts of the Greenland Sea gives us a clue as to how the Greenland Sea communicates with the Norwegian Sea and the Polar Ocean. The resemblance between the water in the Norwegian Sea and the water over the

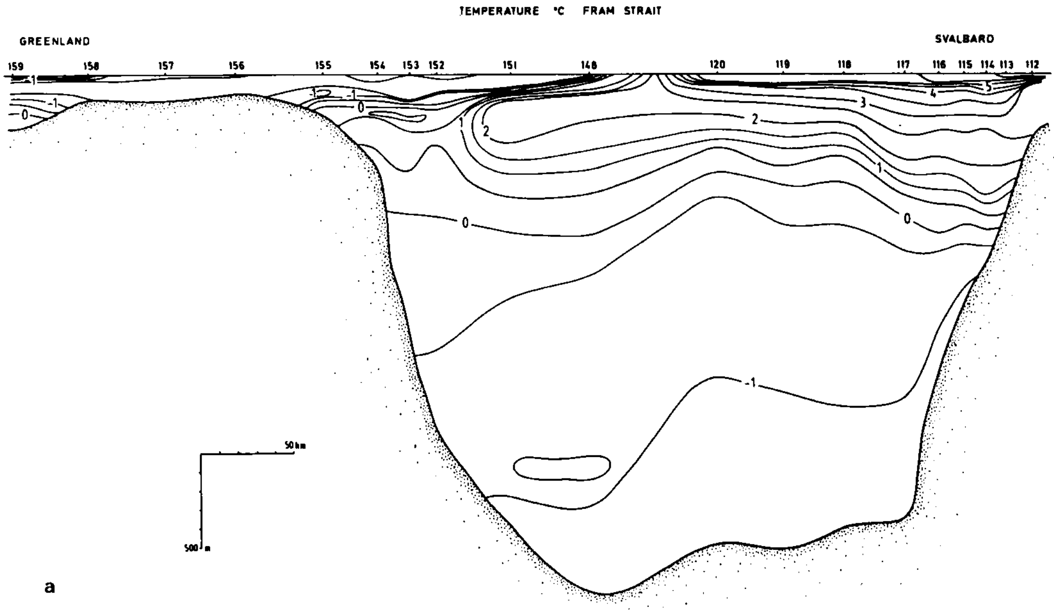

a

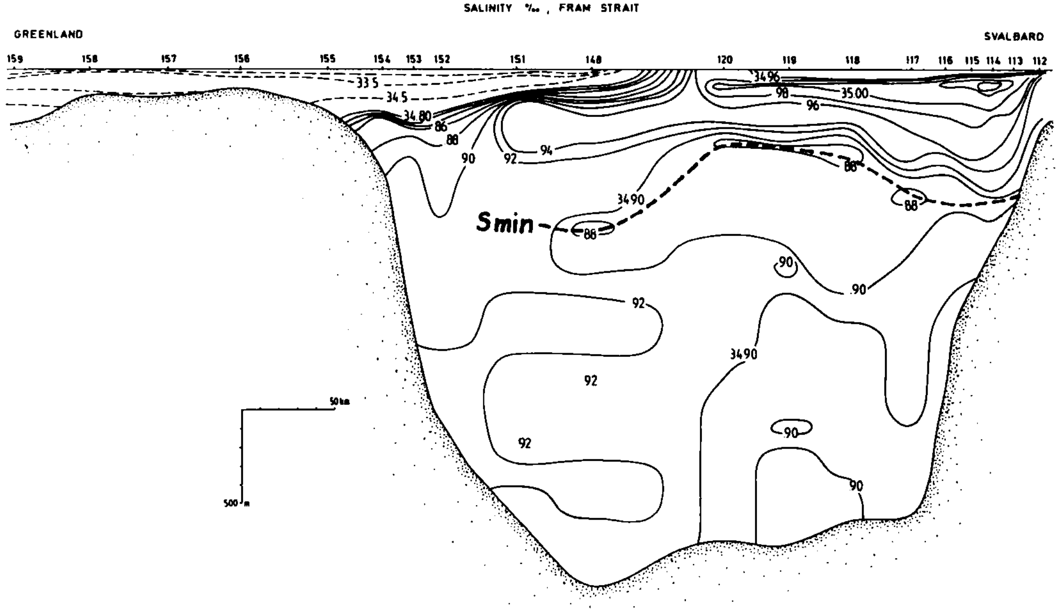

b

Fig. 7a. Potential temperature section across the Fram Strait taken in August 1980 from HMS 'Ymer'. *b*. Salinity section across the Fram Strait taken in August 1980 from HMS 'Ymer'. Salinity minimum indicated.

Greenland slope (Figs. 4c, 6b) suggests that there might be an eastward flow, perhaps close to the Jan Mayen area, which feeds this water from the Polar Ocean into the Norwegian Sea, after its salinity maximum has been removed, or at least lessened by a continuous isopycnal mixing between waters on the slope and in the interior of the Greenland Sea. Such a flow scenario is proposed by Aagaard et al. (1985). This eastward flow is strengthened close to the bottom by the outflow of GSDW through the Jan Mayen fracture zone, which makes up the deepest part of the NSDW (Sælen priv. comm.).

However, one difference between these water masses is that the NSDW is saltier in the temperature range $-0.5°C < \theta < 0°C$. This could be the result of a vertical salt flux from the Atlantic water entering the Norwegian Sea from the south. Another reason might be that this 'upper' low saline water does not take part in the proposed eastward circulation but instead continues southward in the East Greenland Current and enters the Iceland Sea. At any rate we note that the range $-0.5°C < \theta < 0°C$ is much less represented in the eastern than in the western part of the Fram Strait (Fig. 7a). This may be the result of loss of water in this range to the Iceland Sea between Jan Mayen and Greenland.

The subsequent fate of this water, classified as upper AIW by Swift & Aagaard (1981), south of Jan Mayen is not clear. It could pass south through the Denmark Strait or return eastward to the Norwegian Sea, acquiring salt in the process.

Moreover, it is interesting to observe that there is a salinity minimum in the temperature range $-0.5°C < \theta < 0.5°C$ in most of the Fram Strait (Fig. 7b). This minimum may derive from the polar outflow, but it could also represent water created in wintertime in the Greenland Sea, which is then advected northward into the Fram Strait (see section 2).

Stations taken at different latitudes in the Fram Strait (Figs. 8a–c) as well as the stations from the interior of the Greenland Sea and the Polar Ocean (Figs. 6c, 4e) indicate that there exists a deep water exchange through the central part of the Fram Strait. The PODW and the GSDW are both present, at least in the western part of the Fram Strait, and the rugged appearance of the θ–S curves in the deeper layers reveals strong interleaving between these water masses. The intrusions are probably in the last instance removed by double diffusive processes, and the GSDW, which penetrates north into the Polar Ocean, thus acquires θ–S characteristics close to those of the deep NSDW.

Further south we observe a gradual disappearance of the Polar Ocean deep salinity maximum. Still, signs of a maximum remain in the Greenland Sea, where a deep layer slightly saltier and warmer than the bottom water is found. This maximum can be looked upon as the product of isopycnal mixing between newly formed GSDW and PODW from the Eurasian basin.

3. Vertical convection and formation of deep water

We have examined the θ–S characteristics of the deep waters in the different basins following a route which, we believe, approximates the motion of the deep water. We have also commented upon the observed changes of θ–S properties in the water masses. Now we shall turn our attention to the different areas where we expect vertical convection to occur and discuss the possible mechanisms which may be instrumental in promoting the observed changes. This discussion is speculative, and several of the suggested processes require a more thorough treatment than they are given here to be confirmed or rejected. To our mind, however, the picture of the circulation which emerges is consistent. By presenting the different areas together, the differences and similarities are more clearly seen than in a more detailed study.

The effects of the heat loss at the sea surface on the water column are different in the Polar Ocean and in the Greenland Sea.

In the Polar Ocean the salinity increases with depth, and a salinity maximum appears at the bottom. This salinity increase must be the result of brine rejection over shallow areas, which permits a gradual increase of salinity of the water column.

By comparison, the deepest, most dense layer in the Greenland Sea is fresh and cold, giving the impression that cooling, rather than salt supply through brine release, is the dominating effect of the density increase.

The θ–S relations (Figs. 4e, 6c) resemble those observed in the Ross and Weddell Seas respectively (Gordon 1971). The situation seems rather more complicated in the Arctic than in the Ant-

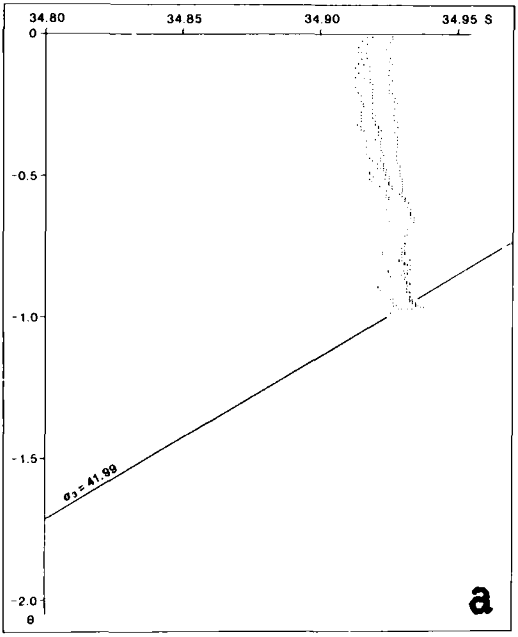

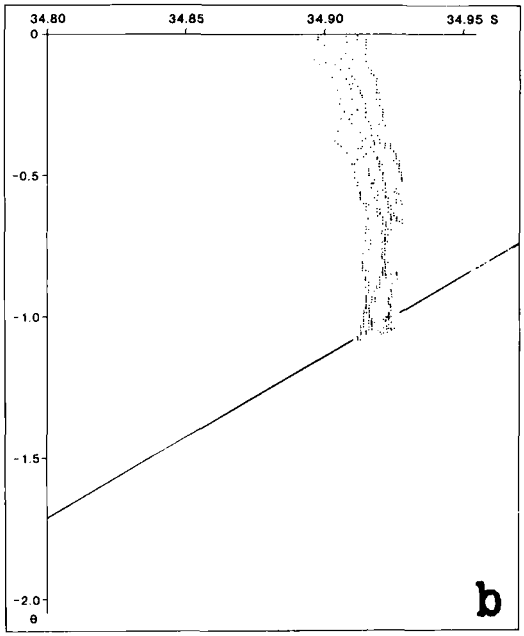

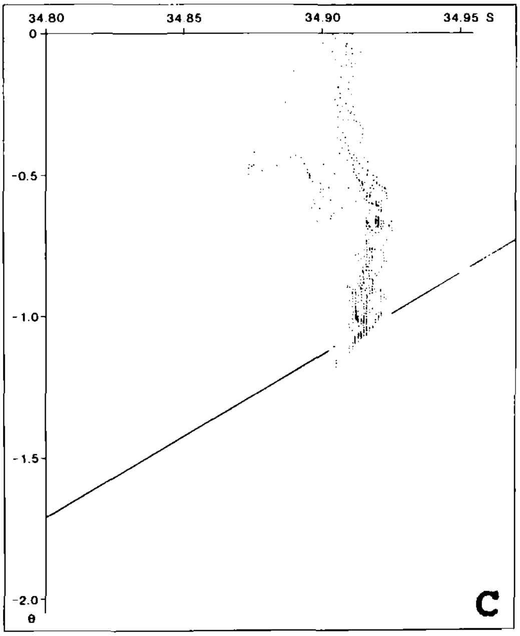

Fig. 8a–c. *θ–S* curves from stations taken at different latitudes in the deeper parts of the Fram Strait. a. Stations Y-166, Y-168, Y-170 from the northern part of the Fram Strait. b. Stations Y-175, Y-176, Y-177, Y-178 taken in the central part of the Fram Strait. c. *Stations* Y-122, Y-148, Y-150, Y-151 *taken in* the southern part of the Fram Strait.

arctic. Here the bottom water with the higher salinity, which ought to be created in connection with ice formation and thus be at freezing point, actually has higher temperatures than the fresher deep water in the Greenland Sea. Moreover, in the Greenland Sea we have no possibility to supercool water at higher pressure, as occurs through melting beneath the Filchner ice shelf in the Weddell Sea (Weiss et al. 1979). To our mind these contradictions depend on the environment in which the cooling and freezing occur – the water depth, and the temperature and salinity of the intermediate layers which the dense sinking plumes have to bypass to enter the deeper waters.

Our guiding picture is therefore the same for the two seas. Dense water is formed at the surface and sinks through the water column to its appropriate density level while mixing with the surrounding waters. Such a process would gradually transform the descending water as well as the water column in the basin. Since we, perhaps unwarranted, assume stationary conditions, the input from the convection must be balanced by an advective inflow from a neighbouring basin to maintain the observed θ–S structure. The corresponding outflow from the basin has the stationary θ–S characteristics of the resulting water column and acts in turn as the advective inflow in the next adjacent basin.

Moreover, we believe that sea ice formation is essential if the high densities required for the convection water to reach the bottom are to be created, both in the Polar Ocean and in the Greenland Sea. This may be somewhat easier to accept for the Polar Ocean than for the Greenland Sea. In section 3.2 below we will account for one reason to embrace such a view. However, first we direct our attention to the Polar Ocean.

3.1. *Deep water renewal in the Polar Ocean*

The principal problem in the Polar Ocean is: If the increased salinity in the deep water is due to the injection of dense brine enriched water at its freezing point from the shelves, why is the temperature of the deep water higher than in the Greenland and Norwegian Seas? That the Atlantic layer should act as a combined source of both heat and salt, preferably through the salt finger process, is unlikely, since this layer constitutes a salinity maximum only in the vicinity of the Fram Strait. The only remaining possibility is that the descending water acquires the necessary heat from entrainment of intermediate water. Thus, the questions are: What changes should be expected in the descending plume? What are the relative proportions of shelf water and entrained intermediate water, and what are the θ–S characteristics of the waters which enter the deeper layers? To try to answer these questions we first turn to the Canadian basin.

3.1.1. *The Canadian basin.* – Due to the presence of the Lomonosov ridge no water deeper than about 1,600 m enters the Canadian basin from the Eurasian basin. The salinity of the water at that level in the Eurasian basin is ~34.92 (Aagaard 1981). By contrast the salinity in the Canadian basin below the sill level is about 34.95 (Aagaard 1981; Aagaard et al. 1985) and dense, saline water must be introduced into the deeper layers.

The strong vertical density gradient in the interior of the Polar Ocean prevents an open ocean deep convection, and the dense water must be formed on the shelves. Because of the shallow depth and the existence of a lower physical boundary a large range of salinities may be attained at different localities during the winter. The production of saline water (and ice) is promoted by the initial absence of ice and the possibility that the prevailing winds may create areas with open water and excessive ice formation (Aagaard et al. 1981; Schumacher et al. 1983).

The dense shelf water will eventually move off the shelves and sink into the deeper parts of the basin. The physics of such a descending plume is discussed at some length in Aagaard et al. (1985). It cannot be decided at present whether there are a few salinity stratified plumes, sinking at preferred sites and gradually becoming 'shaved off', at various density levels, or if the number of plumes is larger and they have their distinct initial salinity which changes during the descent with the amount of entrained ambient fluid.

We have assumed the existence of several plumes with different initial salinities, which sink to their terminal level and then spread out. The amount of entrained water will depend upon the depth of descent and thus upon the initial salinity. Since we expect the plume to be turbulent, the ambient water will mix into the plume with the water from the shelf and the θ–S characteristics of the plume will integrate the characteristics of the ambient water masses to the initial shelf water signature. The denser the initial plume, the more ambient fluid it will have incorporated when it reaches its terminal density level, which of course will be affected by the entrainment. Depending upon the initial salinity on the shelves, the descending water will penetrate down and affect different layers of the water column. The evolution of the θ–S signature of the water particle as it descends through the water column may be indicated on the θ–S diagram. If the initial salinity is low the particle will only pass through the cold upper layer in the interior, which will reduce its salinity but hardly affect its temperature, before it reaches its appropriate density level. When the

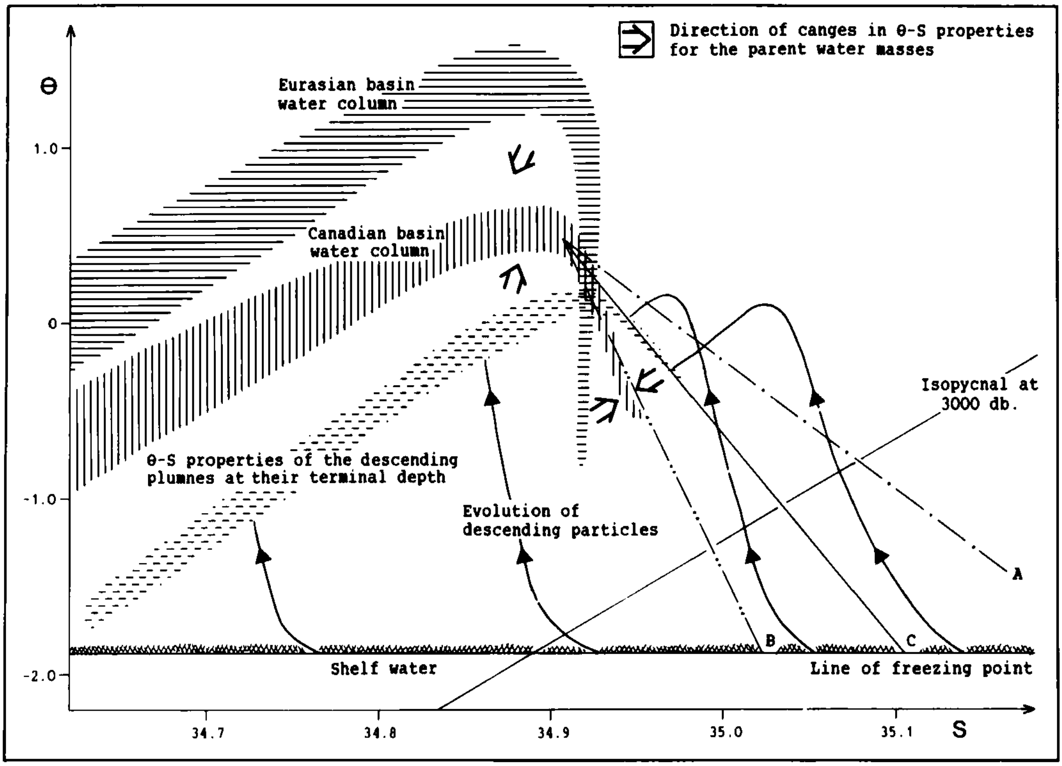

Fig. 9. Transformation of Eurasian basin waters into Canadian basin waters. The water formed on the shelves lies along the freezing point line. For low salinities this water will replenish the halocline when it leaves the shelf. At higher salinities the water intrudes into the Atlantic water and cools it. It may also become dense enough to enter the deep water. The evolution and final θ–S points for the descending plumes are suggested. The ratio of the advective to convective contribution is taken to be 2:1.

salinity is higher it will penetrate through the surface layer into the Atlantic water, and its temperature increases. Finally, for high enough salinities, the water particle passes through both the surface and the Atlantic layer and enters the deep water. The temperature of the particle will pass through a maximum and start to decrease as the colder deep water becomes entrained. The evolution of the θ–S signatures for different initial salinities is indicated in Fig. 9.

Since we expect that all particles which enter the deeper layers have attained the same maximum temperature as they pass through the Atlantic layer, their final temperatures will depend upon the amount and the temperature of the entrained deep water. This implies that there is a minimum temperature which the convective particles can attain. Higher salinities and densities on the shelves will lead to higher salinities but not to lower temperatures in the bottom layer. This explains the constant temperature encountered in the deeper layers of the polar basins.

The θ–S characteristics of the plumes at their terminal density and depth define the θ–S relations of the convective contribution to the basin and are indicated in Fig. 9. As they mix into the water column they will lower the temperatures and salinities of the upper layers, but deeper down the effect will be reversed and the lower layers will become warmer and saltier (Fig. 9).

These changes must, in a steady state, be balanced by an inflow of water from the Eurasian basin (Fig. 9).

We have not tried to apply any of the existing theories on entraining buoyant plumes sinking along a sloping boundary (Killworth 1977; Smith 1975), and the suggested θ–S relations of the convective contributions are quite subjective. However, we have tried to establish the point reaching deepest into the water column. The temperature in the Eurasian basin at the sill depth of the Lomonosov ridge is about 0.15°C lower than the one at the same level and deeper down in the Canadian basin (since the temperature there is constant) (Coachman & Aagaard 1974). The deep water in the Canadian basin has approximately the same density as the water at sill level in the Eurasian basin, and we assume that the advective inflow from the Eurasian basin and the convective contribution from the Canadian basin mix isopycnally, forming the Canadian basin water column. Since the θ–S characteristics of the water column are taken to be stationary, these contributions must balance, and by continuing along the isopycnal connecting the densest Eurasian basin water capable of crossing the Lomonosov ridge with the densest Canadian basin water, we should encounter the point representing the contribution from the convection in the Canadian basin.

Taking the water at the temperature maximum to approximate the entrained fluid which mixes with the descending shelf water with temperature at freezing point, we could, provided we knew the salinity of the shelf water, find the θ–S characteristic of the intruding plume. Unfortunately, this is not the case and we must make some guesses.

High salinity of the shelf water would demand a large contribution from entrainment and a large advective contribution (Fig. 9, line A). Since the intermediate water is incorporated into the convective contribution, this implies a larger inflow of deep water than of intermediate water from the Eurasian basin. On the other hand, a low shelf salinity implies a smaller entrainment but requires a much stronger convection as compared to advection. This means a large inflow of intermediate water but a small flow of deep water close to the sill (line B).

We expect the inflow of intermediate and deep water to be of equal magnitude, which suggests a ratio of the advective to convective contributions of 1 : 1 (line C). This implies a salinity of about 35.1 for the shelf water and a ratio of 2 : 1 between entrained water and shelf water. However, this may be an underestimate since cold water is entrained as well.

The value 35.1 for the shelf water with the same mixing ratio was also found by Aagaard et al. (1985) based upon somewhat different argumentation.

Before turning to the Eurasian basin we observe that if we were considering a salinity stratified 'shaving plume' as in Aagaard et al. (1985), the intruding fluid would act to lower the temperatures at all levels and a cold saline bottom water would result. Whether this really is the case cannot be decided from the observations available for the Canadian basin.

3.1.2. *The Eurasian basin.* – In the Eurasian basin there is also a salinity increase in the deep and bottom water. It is found at deeper levels, however, and appears more prominent in the θ–S diagrams (Fig. 4e). It is likely that a similar mechanism is active here, as was suggested for the Canadian basin.

Another explanation is possible, however. The Atlantic water is close to the surface in the area north of Svalbard and may by direct cooling attain temperatures and salinities necessary to produce the observed changes in the deeper layers. Still it is hard to see how such cooling would concentrate the largest salinity changes to the deepest part of the water column. One would rather expect a uniform increase in salinity and temperature over the entire lower part of the water column.

However, the open water often observed north of Svalbard indicates that the water there is warm enough to prevent ice forming and maintaining a large heat loss. The question is whether this heat loss is sufficient to create water dense enough to replenish the bottom layers. To cool the 400 m thick Atlantic layer from +3°C to −1°C would require a heat loss of 400 W/m^2 during a six month period, which is unlikely. The cooling must occur over shallow areas.

It should be remembered that the most effective way by far to create dense water is to increase its salinity. Even if the Atlantic water has high initial salinity, its temperature is also comparably high and cooling will lower its temperature but may not change its salinity. Therefore cooling may not increase its density sufficiently.

To be specific: Consider a 60 m deep shelf. A heat loss of 60 W/m^2 in six winter months is enough to lower the temperature of the Atlantic water from +3°C to −1°C. The same heat loss would also form 3 m of ice and increase the salinity by 1.5 if the shelf instead were covered with polar water with a temperature close to freezing point. Polar water with salinity of 33.5 and density $\sigma_\theta \sim 27.0$ would attain a salinity of 35 and a σ_θ of 28.15 as compared to a σ_θ change from 27.90 to 28.12 for the Atlantic water.

There are indications that cooling and freezing occur in the northern and eastern Barents Sea and perhaps over the shelf area north of Svalbard. The temperature minimum found in the halocline at 75–100 m with temperatures at freezing point suggests that it could be formed over shallow shelves rather than by local convection. Deeper in the Atlantic layer there are cold intrusions, which would be the result of still larger ice formation. These intrusions will eventually be removed by double diffusive convection and could be the main mechanism for cooling the Atlantic layer in the Polar Ocean.

The Atlantic water also enters the Polar Ocean over the Barents Sea. This inflow may be comparable to the one through the Fram Strait (Rudels 1986), and it probably supplies most of the water to the polar surface water and the halocline, but it may also become dense enough to penetrate deeper into the water column (Fig. 2b) (Swift et al. 1983).

However, even if AW cooled in the Barents Sea may become dense enough to influence the deepest layers in the Polar Ocean, the densest waters observed in the Barents Sea – in the eastern depressions and in the Storfjorden area – have been at freezing point with salinities above 35 (Nansen 1906; Midttun 1985), thus indicating that even in these parts, close to the saline inflow from the Atlantic, ice formation is required to create really dense water.

We then assume that brine rejection is the most important mechanism for convective renewal inside the Eurasian basin, and we propose the same mechanism as for the Canadian basin. But in the Eurasian basin transports from the Greenland/Norwegian Seas together with the convection in the Eurasian basin keep the θ–S characteristics of the Eurasian basin deep water in a steady state.

The inflow through the Fram Strait more resembles the NSDW than the GSDW, and we take the θ–S characteristics of the NSDW as representative of the advective contribution (Fig. 10).

The larger temperature range for the deep waters in the Eurasian basin complicates the interpretation of the mixing since the final θ–S characteristics of the densest plumes will to a large extent be due to entrainment of deep water. We have therefore tried to describe the evolution of the descending water particles through the temperature maximum to their final θ–S characteristics to estimate when the entrainment of deep water ($\theta < 0$) commences for the different water particles. The curve connecting these points is indicated in the θ–S diagram, and the θ–S relation represented by the curve is then used as the convective contribution which mixes with the inflowing NSDN (Fig. 10). Since the water particles on the curve have not attained their final θ–S characteristics, the mixing between the descending water and the NSDN will not be along the isopycnals on the θ–S diagram. The ratio of the advective to the convective contribution is estimated from the EBDW θ–S characteristics between the curve and the NSDN, and we put the ratio at 8:1.

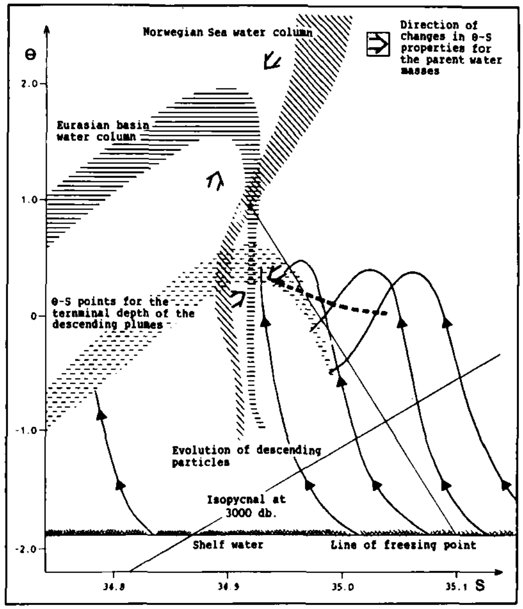

Fig. 10. Transformation of inflowing Norwegian Sea and Greenland Sea waters into Eurasian basin waters. Broken line indicates when deep water begins to be entrained into the plumes. Assumed advective to convective contribution 8:1.

The ratio of entrained intermediate water to shelf water appears to be close to 2:1 just as was found in the Canadian basin, and the average shelf water salinity is estimated to 35.1 (Fig. 10).

It thus appears that advection dominates over convection in the Eurasian basin, while the two contributions are more balanced in the Canadian basin. So far we have only established ratios, not rates, and it is not possible to ascertain if the formation of dense saline water on the shelves is less extensive in the Eurasian than in the

Canadian basin. This would seem strange, since we are here closer to the principal salt source, the Atlantic. On the other hand, convection to the bottom would require higher densities in the Eurasian basin and may be limited on that account. Also the heat stored in the Atlantic water may reduce the ice formation in areas like the Barents and the Kara Seas and make them less favourable for deep water formation than one would have reason to expect.

Another, perhaps more obvious reason would be that the advective contribution from the Fram Strait is much stronger than the corresponding flow across the Lomonosov ridge. We shall return to these questions in section 4 below, after having examined the conditions in the Greenland Sea.

3.2. *The Greenland Sea*

In the Greenland Sea the active area, where the convection is expected to occur, is over the deep central gyre (>3,000 m), where the vertical density stratification is almost wholly absent. An actual convection has so far not been observed in the Greenland Sea whereas it has in the Mediterranean and Labrador Seas (Stommel 1972; Clarke & Gascard 1983; Gascard & Clarke 1983), if by a convective event we mean a situation where a homogeneous water column is observed reading from the surface deep down towards the bottom. There may be several reasons for this; lack of observations, intermittent formation in time as well as in space, no deep and bottom water may be formed at the present time.

But perhaps we should be looking for something else, not a homogeneous water mass, but rather signs of interleaving waters with different θ–S characteristics. Such interleaving is frequent in the central Greenland Sea gyre and is most readily explained as remnants of sinking particles, which have reached their density levels. These intrusions cannot prevail for long in view of double diffusive effects. Perkin & Lewis (1984) estimate a life time of less than a year for the intrusions observed in the Atlantic inflow to the Polar Ocean. The intrusions thus merge into the dominant θ–S structure which is the result of the combined effects of these convective events and an advective contribution, here as well as in the Polar Ocean.

While its density shows small vertical variations, the water column in the Greenland Sea is far from homogeneous and displays a characteristic θ–S structure. Between about 1,200 and 2,200 m there is a deep cold ($\theta <$ -1.1°C) salinity maximum ($S \sim 34.90$) which is bounded below by the cold fresh GSBW ($\theta \sim 1.28$, $S \sim 34.893$) and above by a slightly warmer ($\theta \sim 1.05$°C) layer as fresh as the bottom water. Above these water masses there is mostly confusion, but various stages of isopycnal mixing between a water mass with constant salinity and a temperature ranging from 0 to 1°C and another water mass located along the line of the temperature of the freezing point could account for the observed structure.

To be able to proceed, we need to identify the θ–S characteristics of the advected contributions from outside the Greenland Sea and the θ–S signature of the water which is formed in the Greenland Sea gyre.

We believe that the deep salinity maximum is an advective feature and derives from the outflow of the Polar Ocean. We take this as a clue and postulate that the deep water advecting into the Greenland Sea gyre is Polar Ocean deep water, entering either directly through the Fram Strait or by mixing between the central gyre and the boundary current leaving the Polar Ocean along the Greenland slope (sect. 2).

The water which is formed in the Greenland Sea gyre must be able to sink through the salinity maximum, entraining water, and still be fresh enough to maintain the low saline θ–S signature of the bottom water. It then has to originate from a rather limited part of the θ–S diagram. It is not possible to lower the temperature and salinity of the maximum, transforming it into bottom water, by any molecular process from above since it is capped by warmer less saline water. If anything occurs down there it would be a vertical saltflux from the saline layer into the bottom water, due to salt fingering, which would act to increase the salinity and temperature of the bottom water.

The thermodynamic processes, which change the θ–S characteristics of the water masses, are most effective at the sea surface, as they are associated with cooling and freezing due to air–sea interaction. We shall therefore look at the possibilities of transforming the surface water in such a way that it enters the area of the θ–S diagram from where it may affect the bottom water.

The effect of cooling is bounded by the line of freezing, and by lowering the temperature the surface water may not at first attain a sufficiently high density to sink into the deeper layers. However, ice formation could make a water parcel move horizontally in θ–S space along the line of freezing into the critical area, where its density approaches that of the bottom water.

We thus opt for the freezing at the sea surface as the mechanism creating water dense enough to sink through the intermediate layer entraining ambient water and replenish the bottom water.

To propose that ice formation drives the deep convection in the Greenland Sea may seem far-fetched, and we will therefore devote some time to discuss the features which we believe are important for the convection before we try to determine the ratio between the different water masses forming the GSDW.

3.2.1. *Convection in the Greenland Sea*. – To add fresher water at the freezing point is not a new idea and it resembles the mechanism proposed by Foster & Carmack (1976) for the bottom water formation in the Weddell Sea. This process was in principle vindicated by the isotope work by Weiss et al. (1979), which showed the presence of ice shelf water in the bottom water. The seemingly fresh bottom water found in the Weddell Sea is thus the result of a shelf process, albeit one of melting rather than freezing. The process produces water at the freezing point which 'draws' the θ–S characteristics towards colder fresher values.

In the Greenland Sea the situation is complicated by the absence of a physical lower boundary which could trap the water and thereby make its density increase above that of marginal stability. The final depth of the convection will of course be a compromise between the ambient stratification, entrainment and the initial density anomaly of the convecting element. It could in principle be obtained from a theory for the entrainment of the surrounding waters into the descending elements, provided that the initial density anomaly were known. The question then becomes: How large a density anomaly may be accumulated before the particle leaves from the sea surface, and what would be the dimensions of the sinking particles?

With winter temperatures close to the freezing point, heat loss at the sea surface will result in ice formation rather than a cooling of the surface layer. The removal of fresh water increases the salinity and density of the surface layer, and a gravitationally unstable situation develops.

In passim we may note that the removal of water by evaporation instead of freezing effectuates a density increase due to a lowering of temperature rather than to a salinity increase because of the large heat of combustion. Thus, it more resembles a cooling than a freezing process.

We shall consider a highly idealized situation with no mechanically generated turbulence present in the surface layer. This is an obvious oversimplification, and it might only occur in water beneath land-locked ice. Below we shall comment briefly on what effects should be expected, if wind generated turbulence is taken into account.

The gravitational instability at the sea surface is created by molecular diffusion, and the small convecting elements cannot penetrate far into the water column before their density anomaly is again removed by the diffusion of salt into the surrounding water mass. This in turn results in a redistribution of dense water over a larger volume which eventually must sink into the water column. In the absence of externally generated turbulence we believe that the size and density anomaly of this 'second' convection must and could be found by examining the first, molecular process.

The scale of instability created by molecular processes is given by the penetration depth δ of the heat loss (Howard 1964)

$$\delta \sim (\pi k_\tau t)^{1/2} \tag{1}$$

where k_τ is the coefficient of heat diffusion and t the elapsed time. For a given heat loss Q an equivalent amount of ice will be formed, resulting in a density increase $\Delta\rho$ given by

$$\Delta\rho = \beta\left(S - \frac{S(\pi k_\tau t)^{1/2}}{((\pi k_\tau t)^{1/2} - Q(\rho L)^{-1} t)}\right) \tag{2}$$

S is the salinity, L is the heat of fusion and β is the coefficient of salt contraction.

It is assumed that sea ice is formed when the cooling is felt and the ice crystals are brought to the upper boundary, leaving only the salt excess in the affected volume. This process takes a finite time and we will therefore overestimate the density anomaly and underestimate the time needed for the instability to become critical (see below). Since a gradient is needed for the penetration of the cooling we must allow for some supercooling before the ice crystals begin to form. However, it is k_τ not k_s, which must be used to find the dimension of the unstable particle.

The growing instability may then be described by a Rayleigh number

$$Ra = \frac{g\Delta\rho\delta^3}{\rho k_s \nu} \tag{3}$$

based upon the penetration depth, the density anomaly and the coefficient of salt diffusion k_s, since it is the diffusion of salt, not heat, which may prevent the instability from becoming critical. ν is the coefficient of viscosity.

If a turbulent mixed layer is taken into account, the ice formation will occur inside the well mixed layer (Omstedt 1985), and the description given here will not be valid. Ice crystals will then form immersed in warmer, saline water particles, due to the release of latent heat and the rejection of salt. The heat will be rapidly removed by diffusion, leaving the ice crystal and the excess salinity virtually unchanged. The ice and the water particle will then separate due to their different buoyancies – the crystal rising and the water particle sinking. The vertical scale of the 'secondary' instability would in this case probably be determined by the depth of the wind mixed layer. Taking the time needed for an ice crystal to rise through the layer as the time necessary for the instability to become critical, we would obtain the size and density anomaly of the sinking elements.

To determine the depth of the wind mixed layer we must know the wind speed and cooling rate and have a theory for the development of a negatively buoyant Ekman layer. We also need to know the size of the ice particles to find their transit time to the surface. Rather than indulge in an excess of estimates, we have chosen to ignore external factors (except cooling) and to concentrate on the molecular processes.

When the critical Rayleigh number Ra^* is reached the unstable particle starts to convect and the time t^* needed for the instability to become critical can be found from

$$Ra^* = \frac{g\beta S\left(\frac{(\pi k_\tau t^*)^{1/2}}{(\pi k_\tau t^*)^{1/2} - Q(L\rho)^{-1}t^*} - 1\right)(\pi k_\tau t^*)^{3/2}}{\rho\nu k_s} \tag{4}$$

which gives

$$t^* = \left(\frac{Ra^*\rho\nu k_s((\pi k_\tau)^{1/2}L\rho - Qt^{*1/2})}{g\beta SQ\,(\pi k_\tau)^{3/2}}\right)^{1/2} \tag{5}$$

The average heat loss in the Greenland Sea during the coldest winter months is about 200 W/m^2, and during exceptional cooling events we may expect it to be higher. Tentatively, we shall use the values 300 W m^{-2} and 500 W m^{-2}.

To decide upon a representative Rayleigh number is more difficult. The shape of the density profile is far from linear and the finite time needed to remove the ice complicates the issue. We have tried to take the time needed for the ice formation and ice removal into account by adopting a value $Ra^* \sim 10^4$ since we expect the presence of ice to inhibit the instability. Note, however, that the depth of the penetration and the density anomaly should hold, since we assume that the ice will eventually leave the descending particle during the acceleration phase. Using $\beta \sim 8 \,.\, 10^{-4}$ g/cm^3, $\nu = 0.015$ cm^2/s, $k_\tau = 0.001$ cm^2/s, $k_s = 0.00001$ cm^2/s and $g = 1000$ cm/s^2, the value of t^* is found by iteration, and

$t^* = 13.8$ s; $Q = 300$ W m^{-2},
$t^* = 10.7$ s; $Q = 500$ W m^{-2}

and the corresponding penetration depths, density and salt anomalies are

$\delta^* = 0.21$ cm	$\delta^* = 0.18$ cm
$\Delta s^* = 0.21$	$\Delta s^* = 0.31$
$\Delta\rho^* = 0.00017$ g/cm^3	$\Delta\rho^* = 0.00025$ g/cm^3

The dense particles sink from the boundary, and if they are approximated by spheres with radius $\frac{\delta^*}{2}$ subject to Stoke's resistance law we may write the velocity W of the descent as (Batchelor 1967; Turner 1973)

$$W \sim \frac{g\Delta\rho^*\left(\frac{\delta^*}{2}\right)^2}{3\rho\nu} \tag{6}$$

and we get

$W = 0.04$ cm/s; $Q = 300$ W/m^2,
$W = 0.05$ cm/s; $Q = 500$ W/m^2

The terminal depth Z reached by the particles depends upon how fast the density anomaly is removed by diffusion. Since the rate of diffusion is proportional to the surface area of the particle we have (Turner 1973)

$$\Delta\rho \sim \Delta\rho^* \exp-(k_s t/\pi\delta^{*2}) \tag{7}$$

which gives

$$Z = \frac{g\Delta\rho^*\pi\delta^{*4}}{12\rho k_s \nu} \tag{8}$$

and we obtain

$z = 450\,\text{cm};\ Q = 500\,\text{W/m}^2,$
$z = 580\,\text{cm};\ Q = 300\,\text{W/m}^2$

The dimensions of the particles are larger and their density anomalies and sinking velocities less than the values given by Wakatsuchi (1983) in his study of convection beneath growing ice. This is not surprising since we are ignoring the processes inside the ice sheet which lead to the later draining of the brine. The smaller velocity could partly be due to our treatment of the saline particles as 'thermals' rather than as laminar plumes. The particles also become more saline with rapid cooling, contrary to Wakatsuchi's result. This is probably due to our neglect of the trapping of brine in the ice with faster cooling.

As long as the saline particles retain their identity, they will sink through an environment which is neutrally stratified or weakly stable. Not until the salinity anomaly has diffused and merged with the surrounding water does this larger volume become dense and unstable with respect to the underlying water masses. As an estimate of the time needed for this diffusion to take place we use the e-folding time $t_0 \sim \dfrac{\pi\delta^{*2}}{k_s}$ which leads to

$13{,}500\,\text{s};\ Q = 300\,\text{W m}^{-2},$
$10{,}200\,\text{s};\ Q = 500\,\text{W m}^{-2}$

for the values obtained above. If the velocity of the particles is assumed constant during that time we find for $Z_0 = Wt_0$ that

$Z_0 = 550\,\text{cm}\ Q = 300\,\text{W m}^{-2},$
$Z_0 = 500\,\text{cm}\ Q = 500\,\text{W m}^{-2}$

which roughly corresponds to the terminal depth arrived at above.

The density anomaly of this larger layer is then given by

$$\Delta\rho_0 = \frac{\Delta\rho^*(\pi k_\tau t^*)^{1/2} t_0}{Z_0 t^*}$$

or

$$\Delta\rho_0 = \Delta\rho^* \left(\frac{\pi k_\tau}{t^*}\right)^{1/2} \frac{t_0}{Z_0} \qquad (9)$$

and $\Delta\rho_0$ becomes for the two cases

$Q = 500\,\text{W m}^{-2};\ \Delta\rho_0 = 0.00009\,\text{g/cm}^3,$
$Q = 300\,\text{W m}^{-2};\ \Delta\rho\ = 0.00007\,\text{g/cm}^3$

with the corresponding salinity changes

$\Delta S_0 = 0.11$ and 0.09.

If the entire unstable layer leaves the surface as a thermal after the time t_0 its velocity becomes

$$W_0 \sim (g\Delta\rho Z_0)^{1/2} \sim 6.7\,\text{cm/s} \qquad (10)$$

from Scorer (1978). All of the salt in the sinking brine will not have diffused into the surrounding water volume after t_0, but it will be trapped inside the descending volume and eventually add its density anomaly.

To find how such a two stage convection may appear in the Greenland Sea we use the profile from Stn. 58 taken by Hudson in 1982 (Clarke et al. 1984). A homogeneous 60 m thick surface layer with temperature at the freezing point and with $S = 34.79$ and $\sigma_0 = 28.01$ is found above a weak, about 50 m thick, pycnocline where the density increases to 28.05. Between 125 and 400 m the density remains practically constant and then gradually increases to the 28.08 of the bottom water. If σ_3 (the potential density at 3,000 db) is used, the water column is found to be of marginal stability below 75 m.

For the most rapid cooling a salinity of 34.90 and a density of 28.10 result, which is larger than that of the Greenland Sea bottom water. However, the excess does not seem large enough to bring small 5–10 m entraining thermals deep into the interior.

If, on the other hand, the upper 50–100 m first recirculate as a filling box (Baines & Turner 1969) increasing the density of the surface layer to the $\sigma_0 = 28.05$ of the layers below, which would require 24–48 hours, a σ_0 of 28.14 would then be reached at the surface. Such a thermal might have enough excess density to pass through an environment with a density range of 28.05–28.08, entraining ambient water, and still reach the deepest layers.

A particular feature arising with this kind of convection is that of the compensating upward flow which will be weak close to the surface. Not until the thermals have descended some hundred metres will they have increased so much in size from entrainment that the required return flow is as intense as the convection. This implies that the water masses will be mixed more thoroughly in the deeper layers, in spite of the larger distance to the energy source, than close to the surface where the water will retain an individual signature. This could be one reason for the failure so far to observe a homogeneous convecting water column in the central Greenland Sea.

If the convection is allowed to run for a long enough time, water with temperatures above freezing point will be brought to the surface, and we shall examine if any changes are likely to occur.

The heat capacity of water is $C_p = 1$ cal/g degree and if we use the same approach as when considering the salinity changes we may write

$$\rho C_p \Delta T = \frac{Qt}{(\pi k_\tau t)^{1/2}} \tag{11}$$

where we have distributed the heat loss over the penetration depth.

The Rayleigh number is given by

$$Ra = \frac{g\alpha (C_p\rho)^{-1} \dfrac{Qt}{(\pi k_\tau t)^{1/2}} (\pi k_\tau t)^{3/2}}{\rho \nu k_\tau} = \frac{g\alpha Q \pi t^2}{C_p \rho^2 \nu} \tag{12}$$

and solving for t we obtain

$$t = \left(\frac{Ra \rho^2 C_p \nu}{\pi g \alpha Q}\right)^{1/2} \tag{13}$$

Since no ice particles have to fractionate out of the volume, it may be more realistic to put Ra^* equal to 10^3 instead of 10^4. To compare the brine and temperature driven convections we shall compute t^* for both values. With $Q = 500\ \mathrm{W/m^2}$ we get

$Ra^* = 10^4$; $t^* = 220$ s, $Ra^* = 10^3$; $t^* = 70$ s

The corresponding penetration depths, temperatures and density anomalies then become with $\alpha = -0.8 \,.\, 10^{-4}$ g/cm^3°C.

$\Delta T^* = 3.16$°C $\qquad \Delta T^* = 1.78$°C

$\Delta\rho^* = 0.00025$ g/cm^3 $\qquad \Delta\rho^* = 0.00014$ g/cm^3,

$\delta^* = 0.83$ cm $\qquad \delta^* = 0.45$ cm

Large temperature anomalies are thus connected with an intense heat loss, and unless some supercooling is allowed there is no water mass in the Greenland Sea gyre which could prevent ice formation with this surface heat flux. If the heat loss in some way could be distributed over the larger unstable volume, the heat decrease would become much smaller and ice formation would then not take place.

Using equations 6 and 8 for the vertical velocity and terminal depth we obtain for:

$Ra^* = 10^4$; $W = 0.96$ cm/s, $Z = 2070$ cm
$Ra^* = 10^3$; $W = 0.17$ cm/s, $Z = 120$ cm

and the time for the temperature anomaly to diffuse into the surrounding water becomes for the two Ra^* values

$t_0 = 2150$ s and $t_0 = 700$ s

with the corresponding depths

$Z_0 = 2070$ cm $\qquad Z_0 = 120$ cm

The density anomalies, which accumulate due to cooling are then

$\Delta\rho_0 = 1 \,.\, 10^{-6}$ g/cm^3 and $\Delta\rho_0 = 6 \,.\, 10^{-6}$ g/cm^3
$\Delta T_0 = 0.013$°C $\qquad \Delta T_0 = 0.07$°C

Smaller density anomalies thus arise in the second instability as compared to those resulting from salt release (a factor of 15 if $Ra^* = 10^3$ is used). A convection driven by cooling rather than freezing would then not be able to penetrate as deep as when ice formation is present. On the other hand the upper layer will be ventilated at a much higher rate; its density increases continuously and the convection reaches deeper and deeper. A convection driven by cooling will, even if it occurs in a filling box fashion (Baines & Turner 1969), resemble the more conventional picture of a gradual vertical overturning of the water masses when the critical density is reached, as is found in the Labrador Sea (Clarke & Gascard 1983).

Thus, if the convection in the Greenland Sea, which starts with ice formation, proceeds long enough to allow deeper warmer waters to reach the surface, they might, if further ice formation is prevented, inhibit the deep convection (Killworth 1979). The ventilation will occur on a smaller vertical scale, and the upwelling heat could melt the previously formed ice and all but stop the convection. This could explain the sudden appearance and disappearance of ice covered areas in the central Greenland Sea, but it is only one of several possibilities. The ice may be removed by wind either into the East Greenland Current or out to the Norwegian Sea where it would melt.

3.2.2. *The Greenland Sea water column.* – Accepting the basic mechanisms proposed above – that ice formation at the sea surface is crucial for the deep water formation – we are now ready to assess the ratio of the different water masses which comprise the GSDW. The contributions to the deep water in the Greenland Sea are waters created in the Greenland Sea and distributed along the line of the freezing point in the θ–S diagram

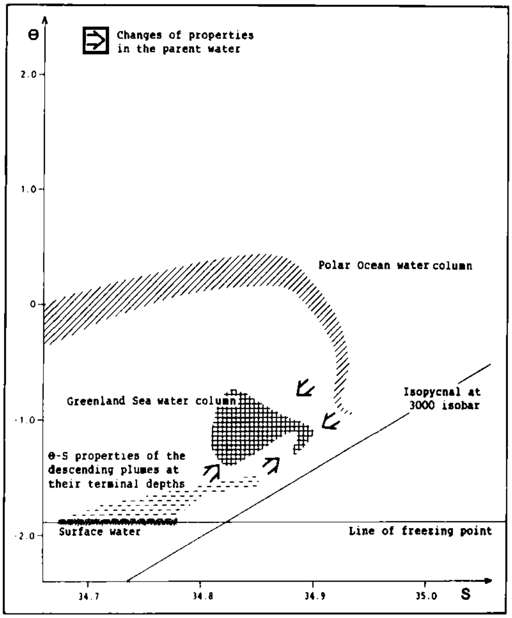

Fig. 11. The formation of Greenland Sea deep water. Water cooled at the sea surface and made saline through ice formation sinks through the intermediate layers. The surface and entrained water together with advected PODW maintain the θ–S structure of the Greenland Sea water column. The ratio of advected to convected contribution is rather arbitrarily taken to be 2:1.

and deep water advected from the Polar Ocean. To maintain the observed θ–S structure in the Greenland Sea we find that a ratio of 1:2 of convected versus advected water is necessary (Fig. 11). Here, since the water column essentially consists of deep water, we will not have any contribution from entrainment.

We have ignored the double diffusive mechanism proposed by Carmack & Aagaard (1973) as a contribution to the Greenland Sea deep water. This is mainly because we believe that inflow from the Polar Ocean rather than from the Atlantic accounts for the deep salinity maximum observed in the central area and that Atlantic water is not present in the deeply convecting region.

The Atlantic water would then mainly pass around the central gyre. But this does not mean that it will not be affected by the cooling at the surface. A convection into the Atlantic water could lead to the situation described at the end of the preceding section, where the water column is cooled and homogenized. At the perimeter of the gyre we would then have a region of what Swift and Aagaard (1981) would call upper Atlantic intermediate water. This is formed at first by a convection into the Atlantic layer triggered by ice formation, bringing it to the surface in a filling box manner, and then by a vertical homogenization due to cooling.

3.2.3. *Estimates of the deep water production in the Greenland Sea.* – The net annual heat loss in the Greenland Sea is from 20 to 40 kcal cm^{-2} (0.8–1.7 . 10^9 J/m^2) (Bunker & Worthington 1976). However, in their discussion of the deep water formation in the Greenland Sea Carmack & Aagaard (1973) suggest a winter heat loss of 75–100 kcal cm^{-2} (3.1–4.2 . 10^9 J/m^2). They also estimate the seasonal cooling of the upper water masses (depth less than 500 m) to be about half this value, or 38 kcal cm^{-2} (1.6 . 10^9 J/m^2), and they take this as evidence for an advective exchange between the Greenland gyre and the surrounding waters.

The observed seasonal changes can be taken as the storing and removal of the summer heating, but these figures only include heat accumulated in the water column, not the heat needed to melt the sea ice either locally formed or advected into the Greenland sea through the northern boundary. Assuming a net ice melt of 1.5 m during the summer, this would require the loss of another 12 kcal cm^{-2} (0.5 . 10^9 J/m^2) and leaving a net annual heat loss of 25 kcal cm^{-2} (1.0 . 10^9 J/m^2). Undoubtedly there are also inflows and outflows of surface waters to the Greenland gyre, but we may expect these to have roughly the same temperature as the exported water and not to change the heat content. 25 kcal cm^{-2} is in the range given by Bunker & Worthington and will be used henceforth. This heat loss is then available to permanently transform water masses in the Greenland gyre.

With a maximum heat loss of 300 W m^{-2} 40 days would be sufficient to remove this heat, and during such a period deep and bottom water may be formed. The formation cannot occur continuously during such a long time span – in that case it would have been observed – but it will be cut off when the sea ice which has been formed becomes thick enough to inhibit the heat loss. This probably happens when the ice thickness reaches 50 cm, which would be after a week of cooling.

We thus expect the surface layer to become gradually denser as the ice forms. After about 2 days it is dense enough for deep water particles to form. These are capable of penetrating deep into the water column (see sect. 3.1.2.). The deep convection will then continue for another five days until the ice cover cuts it off. The ice then has to be removed; it may be driven by the wind into the East Greenland Current area before the convection can start again.

Six such events would be needed to account for the net annual heat loss. During the five days the deep convection is running, about 150 m of transformed water will leave the surface, which runs to a total of 900 m for the winter season.

Carmack & Aagaard give the extent of the Greenland gyre as $0.18 \cdot 10^{12}\,m^2$. Assuming that 10% of this area have a water column dense enough to allow deep water to form, we obtain a formation rate of $0.5 \cdot 10^9\,kg\,s^{-1}$. This is a low but acceptable estimate. The convection would be intermittent in both space and time, but assuming that the intensive cooling occurs during a period of four months, about 1/3 of this area would be actively convecting throughout the period. An even smaller fraction would be needed if higher heat losses occur.

However, the one serious problem with this result is the large net ice production – 3 m – which is demanded and which, with the given heat loss, would take place over the entire Greenland Sea gyre. This occurs because so far we have assumed that the water, after the summer heating is removed, will be at the freezing point with no advective heat flux present. If we take into account the presence of the Atlantic layer, occupying the depth between 200 and 500 m along the perimeter of the gyre, and allow for the possibility of this water to be brought up to the sea surface by the convection, an advective heat flux will take place into the gyre and then to the atmosphere. The Atlantic water can inhibit the ice production by supplying the necessary heat by direct cooling and perhaps also melt ice already formed. This mechanism suggested in section 3.1.2. would be similar to the one proposed by Killworth (1979) for the Weddell Sea Polynya.

If this mixing took place over 2/3 of the Greenland Sea gyre, the net ice production would be reduced to 1 m, which is more acceptable. The Atlantic water would be transformed into 'upper Arctic Intermediate Water' (Swift & Aagaard 1981). If we allow for a cooling of 1.0°C of the Atlantic Water, the formation rate of the AIW could be estimated from energy balance argument to be about $1 \cdot 10^9$ kg/s. This presupposes that the Atlantic water stays more than a year inside the gyre; otherwise a part of the production will show as a seasonal variation, and we will then underestimate the formation rate.

It is thus seen that the proposed mechanisms give acceptable values of the deep water formation. However, the uncertainties, especially about the extent of the area with deep water formation, curtail the results since these could in principle range somewhere between 0 and $4 \cdot 10^9\,kg\,s^{-1}$. We will nevertheless consider a production of $0.5 \cdot 10^9\,kg\,s^{-1}$ of deep water to be the value which best conforms with the present analysis.

4. The circulation of the deep water in the northern basins

Having to the best of our ability determined the ratios of the different water masses making up the deep water columns in the active areas, we shall now try to use these ratios to infer something about the expected circulation in the northern seas.

There are four deep reservoirs in the northern seas, if we separate the Polar Ocean into the Eurasian and Canadian basins. In three of these basins a local renewal of deep water occurs due to cooling and ice formation at the sea surface. The waters which enter the deep layers are described in section 3.

However, to maintain a stationary θ–S structure interaction between convecting waters and the present ambient water masses is not enough. An advective contribution from the neighbouring basins is needed and supplied by the general water circulation of the Arctic Mediterranean.

The deep water is believed to follow a cyclonic path, entering the Polar Ocean on the eastern side of the Fram Strait and then continuing along the Eurasian slope. Some water recirculates in the Eurasian basin, while another part enters the Canadian basin. These two water masses, after being transformed by convection from the shelves, then remerge north of Greenland and constitute the polar outflow through the Fram Strait. Under the influence of local convection, this outflow partly enters the Greenland Sea to form the GSDW and partly bypasses the central Greenland Sea along the Greenland slope while mixing with GSDW. A substantial part of this mixture is assumed to flow east into the

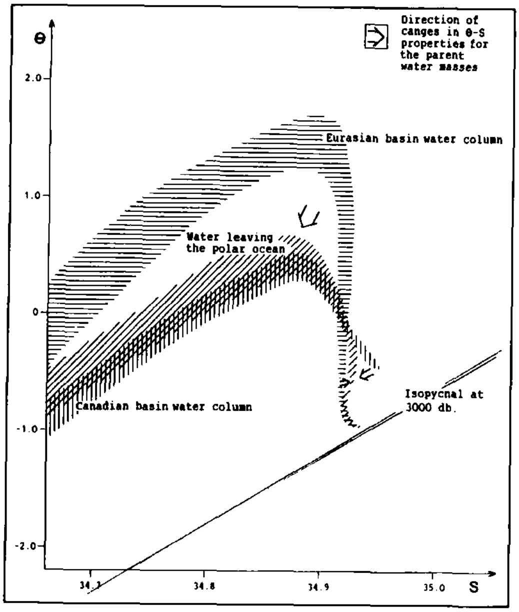

Fig. 12. The waters from the Eurasian and the Canadian basins interacting to form the characteristics of the polar outflow observed in the Fram Strait (surface layer excluded). Tentative ratio 2:1.

Polar Ocean is the result of mixing between EBDW and CBDW (Fig. 12). No CBDW is capable of penetrating and affecting the deepest part of the EBDW mass, but the upper salinity maximum and the lower salinity of the PODW in the vicinity of 0°C can be explained by the presence of water from the Canadian basin where water of that θ–S range occurs. A mixing ratio of 1:2 would account for the lower salinity of the upper salinity maximum than what is found for the deep water in the Canadian basin. The absence of CBDW in the deepest layers could be compensated by a higher percentage in the temperature range 0–$0.5 < \theta < 0$.

The Norwegian Sea deep water is formed by mixing of waters from the Polar Ocean and the Greenland Sea, and again a look at the θ–S curves for the GSDW and the Polar Ocean deep water outflow suggests that an equal mixing of PODW and GSDW would create a water column similar to that of the Norwegian Sea (Fig. 13).

However, we shall parametrize the subsurface mixing in such a way that half of the outflow is exchanged with GSDW which merges with the Norwegian Sea and there form the NSDW which then returns into the Polar Ocean. The deepest part of the NSDW is probably created by outflow of Greenland Sea deep water through the Jan Mayen fracture zone (Sælen pers. comm.), but direct mixing of PODW and GSDW in the western part of the Fram Strait could also contribute to the deepest inflow to the Polar Ocean. This is roughly the scenario presented by Aagaard et al. (1985).

The main ice production and brine rejection occur over the Eurasian and Alaskan shelves, while the area north of Greenland with its thick ice cover probably is inactive in this respect. This implies that both the inflow and outflow of deep water through the Fram Strait are mixture products rather than newly created water masses. The outflow consists of the combined product of waters found in the Eurasian and Canadian basins, and the inflowing Norwegian Sea deep water is comprised by this polar outflow and by Greenland Sea deep water.

Again we try to estimate the contributions from the different basins in these advective flows by comparing the different θ–S signatures.

The θ–S relation of the PODW leaving the

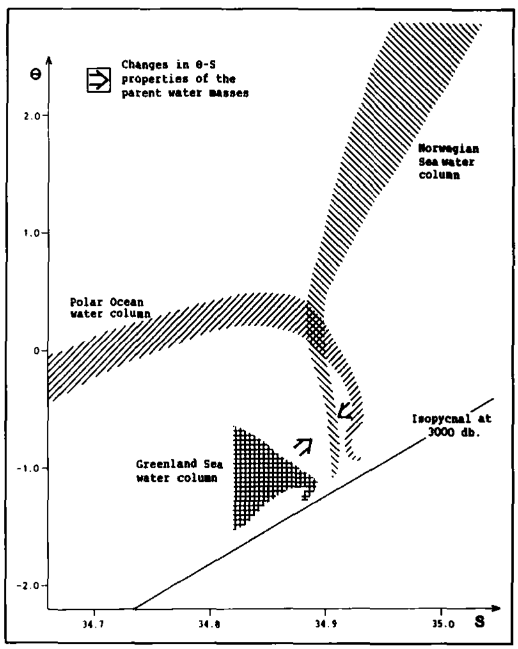

Fig. 13. Formation of Norwegian Sea deep water through isopycnal mixing of PODW and GSDW. The ratio between the water masses is tentatively put as 1:1.

remaining half of the outflow, either on the Greenland slope, creating mainly the upper part of NSDW, or directly in the Fram Strait where a mixing between PODW and GSDW forms a water mass similar to the NSDW.

The exchanged part enters the Greenland Sea, where it acts as the advective contribution necessary to balance the local convection and keep the GSDW θ–S structure stationary. The GSDW then mixes, as was mentioned above, with the PODW in the Fram Strait and on the Greenland slope and also enters directly into the Norwegian Sea through the Jan Mayen fracture zone and over the Mohn ridge.

We are now in a situation to summarize the ratios of the contributions which make up the different water masses:

	advective/convective
Canadian basin DW	1:1
Eurasian basin DW	8:1
Greenland Sea DW	2:1
Polar Ocean outflow	Can. DW/Eur. DW 1:2
Norwegian Sea DW	PODW/GSDW 1:1

Two things should be mentioned with respect to this table.

1. The convective contribution includes both water from the surface and entrained waters. From the discussion of the conditions in the Polar basin we found the ratios of these contributions to be 1:2 if only entrained waters with temperatures above 0°C were considered. In the Greenland Sea the conditions are different. We may expect a larger entrainment since the plumes and thermals will be sinking away from the boundaries. However, almost the entire water mass will be below 0°C and deep water by definition. The entrainment thus creates a redistribution of the deep water, but it will not increase the convective contribution. In estimating the advective/convective ratio for the Greenland Sea we have therefore only used the descending surface water along the line of the temperature of the freezing point as the convective contribution.

2. So far we have only considered sources and not sinks. Some removal mechanism is necessary for mass continuity reasons.

Essentially, two sinks are available. The water may pass into the Icelandic Sea and then exit through the Denmark Strait, or it may acquire a temperature above zero and thus leave our deep water mass by definition. We shall return briefly to this question after we have considered the entire circulation.

It is now possible to relate the ratios in the different basins, and we start by assigning the inflow of NSDW through the Fram Strait the value X Sv.

Inside the Eurasian basin it is augmented by 12.5% and we have $1.25X$ of Eurasian basin DW which splits into one part Y entering the Canadian basin, while the remaining part $(1.125X–Y)$ recirculates in the Eurasian basin.

When the Canadian basin DW returns to the Eurasian basin its volume has doubled to $2Y$, and since the ratio of the Eurasian DW to the Canadian DW in the PODW outflow is 2:1, we get $(1.125X–Y) = 4Y$, which gives $Y = 0.225X$.

The total outflow of PODW thus becomes

$$X + (0.125 + 0.225)X = 1.4X$$

and the deep water circulation has increased by 40% inside the Polar Ocean. Half of this outflow enters the Greenland Sea, while the other half incorporates an equal amount of GSDW and forms the Norwegian Sea deep water.

From the ratio of 2:1 between PODW and the convective contribution we find that $0.35X$ of deep water is formed in the Greenland Sea gyre.

It is seen that about $0.8X$ ought to leave the deep water mass to maintain stationary conditions. If this water exits through the Denmark Strait over the Icelandic Sea it would remove much of the PODW outflow and thus imply a larger part of GSDW in the NSDW amounting to 2:1 instead of 1:1 as has been estimated here. Such a large percentage of GSDW does not seem warranted by the θ–S diagrams, but it might be possible if an additional inflow to the Polar Ocean occurs further to the west in the Fram Strait, where the θ–S characteristics are different from those which we have used for the NSDW and considered representative for the Fram Strait inflow.

In any case our belief is that the excess deep water leaves the system across the Icelandic Sea, perhaps exiting through the Denmark Strait, even if we lack any solid proof to support such a conviction.

We have now reached a point where the θ–S diagram cannot guide us any further. When this work was commenced it was our hope that it would be possible to determine the strength of one of the sources and obtain an absolute value of the circulation. We now realize that this was futile.

Initially, the possibility to estimate the deep water formation rate from heat exchange with the atmosphere was considered. However, in the Greenland Sea the initial temperatures and salinities of the transformed waters are poorly known and the estimates given in section 3.2.3. are very tentative. In the Polar Ocean, where the initial conditions may be easier to determine, a broad spectrum of waters is produced which enters the halocline, the Atlantic layer and the deep water. Since we do not know the relative magnitudes of these products, we cannot proceed further.

The most profitable approach would probably be to estimate the flow through one of the passages, but that is not without complications either. The inflow through the Bering Strait may be well determined, but we can only guess the fraction which will be transformed into deep water. Monitoring the Fram Strait to estimate the strength of the deep water circulation would require extensive current measurements and hydrography work, something that we had hoped to avoid.

What remains is to make a reasonable guess somewhere, and to our mind the best bet would be to turn to the Canadian basin.

The salinities observed in the Chukchi Sea and on the Alaskan shelf are the highest found on the shelves in the Canadian basin. The high salinity indicates an inflow through the Bering Strait distinct from the low salinity water on the East Siberian Sea as well as the Laptev Sea shelves. This comprises a much diluted Atlantic inflow. The shelf water produced in the Canadian basin derives from the Pacific Ocean and considering the limited volume available ($\sim 0.8 \cdot 10^9\ \mathrm{kg\,s^{-1}}$) (Coachman & Aagaard 1981) we believe that no more than 10% or $0.08 \cdot 10^9\ \mathrm{kg\,s^{-1}}$ enter the deeper layers since a comparable amount (at least) must enter the Atlantic layer. Pacific water also constitutes the prime source of the outflow through the archipelago.

0.08 Sv dense shelf water produced in the Canadian basin results in a total contribution of 0.24 Sv to the deep waters in that basin. $\frac{2}{3}$ of the amount is taken to be entrained from the ambient waters. Since $Y = 0.225X$ (see above) we have $X = 1.1$ Sv.

The inflow of deep water through the Fram Strait thus becomes 1.1 Sv and the corresponding outflow is found to be 1.5 Sv. 0.4 Sv of deep water is then produced in the Polar Ocean and perhaps in the Barents Sea. It is again interesting to note that the production of deep water ($\theta < 0$) in the Polar Ocean is twice as large in the Canadian as in the Eurasian basin. This is contrary to what one would believe, and it may indicate that qualitative estimates made from the θ–S diagrams are too uncertain to be really useful. However, we accept our estimate for the time being. Finally, since the amount of deep water formed in the Greenland Sea was found to be 1/4 of the total outflow, we get 0.35 Sv of deep water formed in the Greenland Sea.

To summarize: 0.3 Sv of AW (since both the shelf water in the Eurasian basin and the intermediate layers in the entire Polar Ocean derive from the Atlantic) and about 0.1 Sv of Pacific water are transformed into deep water in the Polar Ocean, which seems acceptable.

The corresponding production in the Greenland Sea (0.35 Sv) seems by contrast surprisingly low but in close correspondence with the result obtained in sect. 3.2.3. It should be remembered though that the actual renewal would be three times this amount or 1.1 Sv since we also have the proposed inflow of PODW.

The seasonal changes of the deep water volume in the Greenland Sea (Carmack & Aagaard 1973; Swift & Aagaard 1981) suggest a production of 1 Sv. This is considerably higher than our estimate since the inflow of PODW would not show up as a seasonal net gain because of the corresponding loss of GSDW to the PODW on the Greenland slope and in the Fram Strait.

One possibility could be that we have ignored the entrainment of intermediate waters in the production of GSDW, assuming that the surface water communicates directly with the deep water. If Atlantic water, which we have taken to be transformed into upper AIW (Swift & Aagaard 1981) at the periphery of the gyre, would be drawn into the centre, a larger volume would be required to balance the influence of PODW on the GSDW θ–S characteristics.

However, it may well be that the θ–S characteristics of the GSDW are not stationary but instead alternate between warmer and colder extremes (Aagaard 1968). Such a varying regime may be understood if two independent sources of GSDW are available. A rapid cooling and a lowering of the deep water temperatures can readily be explained by an extensive local deep water formation due to cooling and freezing. An equally rapid temperature increase is more difficult to visualize unless an inflow of warmer water occurs in the same density range. Such an inflow might be provided by the PODW.

We could imagine a situation where a large heat loss, perhaps associated with cyclonic winds, results in an increased deep water formation, while at the same time the PODW is prevented from entering the central Greenland Sea gyre, either through blocking in the Fram Strait or by being forced up on the Greenland continental slope and thus bypassing the central area.

On other occasions with less or no deep water formation more PODW than usual may penetrate into the central Greenland Sea and increase the temperature of the deep water.

In any case, at this stage we can merely speculate on such possibilities. Nor is there any reason to expect, considering the approximate estimates we have made, that our value for the deep water formed in the Greenland Sea would be closer to other results than a factor of 2–3.

We may thus conclude that about 1 Sv of deep water is formed in the northern basins; it probably exits southward into the Iceland Sea and ultimately into the North Atlantic.

Finally we notice that the exchange of deep water through the Fram Strait is larger than the formation rate. It is an effect of the introduction of the passive water masses, especially the NSDW, which were found necessary to maintain stationary θ–S structures in the different basins. This indicates that the formation of dense water does not primarily drive the deep water circulation. Instead it is forced from above either by meteorological factors or by the density field and the corresponding geostrophic motions in the upper layers resulting from the transformation of Atlantic water into polar surface water inside the Polar Ocean.

5. Summary and conclusion

In the present work the shapes of the θ–S curves observed in different areas have been used to make conjectures about the formation and evolution of the deep water in the northern basins. The estimates of the different contributions have been vague, and the accent has been on approach rather than to obtain exact figures. This view seems justified, considering the rather sparse observations which are available from these areas and our lack of knowledge about the time variability both seasonally and annually. If the approach is fruitful, it can be used anew when more information is at hand.

The use and the form of the proposed convective contributions for the renewal of the deep water may be more questionable. Such sinking water masses have not so far been observed and their assumed θ–S signatures have no theoretical backing but are introduced to explain the observed changes in the θ–S curves.

Finally, to get rates and ratios of the involved mixing components some 'reasonable' guesses had to be made:

1. The average salinity of the water formed on the shelves in the Canadian basin (35.1).
2. The amount of water from the Pacific entering the deep water of the Canadian basin (0.08 Sv).

If these values could be determined by some other means, perhaps utilizing other 'tracer' observations, more reliable estimates of the mixing ratios and the strength of the circulation could be made.

It has not been possible to get any absolute value of the deep circulation through the Fram Strait and the deep water formation in the Polar Ocean and the Greenland Sea. The estimates we have arrived at, about 1 Sv entering and 1.5 Sv leaving through the Fram Strait, and a production of 0.4 Sv of deep water both in the Polar Ocean and in the Greenland Sea, seems reasonable. We hope that this discussion of the θ–S relationship found for the deep waters in the northern basins may have thrown some light on the processes active in basins.

Acknowledgements. – I wish to thank the oceanography teams on board M/S 'Polarsirkel' and HMS 'Ymer' for a stimulating and rewarding time, and especially Arne Foldvik at Geophysical Institute, University of Bergen, making it possible for me to participate in the 'Polarsirkel' cruise and permitting the data to be used in this work. The data from both cruises have been processed at the Geophysical Institute in Bergen.

Thanks are also due to Jorunn Myklebust and Espen Kopperud at the Norwegian Polar Research Institute for their typing of the manuscript and drawing of the illustrations, respectively.

An outline of this work was presented at the ICES Oceanic Hydrography Working Group meeting in Oban. The comments given there as well as suggestions from referees are gratefully acknowledged.

References

Aagaard, K. 1968: Temperature variations in the Greenland Sea deep water. *Deep-Sea Res. 15*, 281–296.

Aagaard, K. 1981: On the deep circulation in the Arctic Ocean. *Deep Sea Res. 28*, 251–268.

Aagaard, K., Coachman, L. K. & Carmack, E. C. 1981: On the halocline of the Arctic Ocean. *Deep Sea Res. 28*, 529–545.
Aagaard, K., Swift, J. H. & Carmack, E. C. 1985: Thermohaline circulation in the Arctic Mediterranean Seas. *J. Geophys. Res. 90*, 4833–4846.
Baines, W. D. & Turner, J. S. 1969: Turbulent buoyant convection from a source in a confined region. *J. Fluid Mechanics 37*, 52–80.
Batchelor, G. K. 1967: *An introduction to fluid dynamics.* Cambridge Univ. Press, Cambridge. 615 pp.
Bunker, A. F. & Worthington, L. V. 1976: Energy exchange charts of the North Atlantic Ocean. *Bull. Amer. Meteor. Soc. 57*, 670–678.
Carmack, E. C. & Aagaard, K. 1973: On the deep water of the Greenland Sea. *Deep Sea Res. 20*, 687–715.
Clarke, R. A. & Gascard, J. C. 1983: The Formation of Labrador Sea Water. Part I: Large Scale processes. *J. Phys. Oceanogr. 13*, 1764–1778.
Clarke, R. A., Reid, J. L. & Swift, J. H. 1984: CSS Hudson Cruise 82–001 14 February–6th April 1982. *Univ. of Cal. Scripps Inst. of Ocean. 84-14.* 2 vols.
Coachman, L. K. & Aagaard, K. 1974: Physical oceanography of arctic and subarctic seas. Pp. 1–72 in *Marine Geology and oceanography of the Arctic Seas.* Hermann Springer Verlag, New York.
Coachman, L. K. & Aagaard, K. 1981: Reevaluation of water transports in the vicinity of the Bering Strait. In Hood, D. W. & Calder, J. A. (eds.): *The eastern Bering Sea Shelf. Oceanography and Resources, vol. 1.* Dept. of Commerce, National Oceanic & Atmospheric Admin., Washington D.C.
Coachman, L. K. & Barnes, C. A. 1962: Surface water in the Eurasian basin of the Arctic Ocean. *Arctic 15*, 251–277.
Foster, T. D. & Carmack, E. C. 1976: Frontal zone mixing and Antarctic bottom water formation in the southern Weddell Sea. *Deep-Sea Res. 23*, 301–317.
Gascard, J. C. & Clarke, R. A. 1983: The formation of Labrador Sea Water. Part II: Meso scale and smaller scale processes. *J. Phys. Oceanogr. 13*, 1779–1797.
Gordon, A. L. 1971: Oceanography of Antarctic waters. Pp. 169–203 in Reid, J. L. (ed.): Antarctic Oceanology 1. *Antarctic Research series 15.* American Geophysical Union.
Helland-Hansen, B. & Koefoed, G. 1907: Hydrographie. Pp. 275–343 in *Croisère océanographique accomplie à bord de la Belgica dans la mer de Grønland 1905.* Duc d'Orléans, Bruxelles.
Helland-Hansen, B. & Nansen, F. 1909: The Norwegian Sea. Its physical oceanography based upon the Norwegian researches 1900–1904. *Rep. on Norw. Fishery and Marine Investigations II(1).* Kristiania.
Howard, L. N. 1964: Convection at high Rayleigh Number. Pp. 1109–1115 in Görtler, M. (ed.): *Proc. eleventh Int. Congress Applied Mechanics.* Springer-Verlag, Berlin.
Kiilerich, A. 1945: On the hydrography of the Greenland Sea. *Medd. om. Grønland 144(2).* 63 pp.
Killworth, P. D. 1977: Mixing on the Weddell Sea Continental slope. *Deep-Sea Res. 24*, 427–448.
Killworth, P. D. 1979: On 'chimney' formations in the oceans. *J. Phys. Oceanogr. 9*, 531–554.
Killworth, P. D. 1981: Deep convection in the world ocean. *JSC/CCCO meeting on time series of ocean measurements, Tokyo.*
McDougall, T. J. 1983: Greenland Sea bottom water formation: A balance between advection and double diffusion. *Deep Sea Res. 30*, 1109–1117.
Metcalf, W. F. 1955: On the formation of bottom water in the Norwegian basin. *Transaction of the American Geophysical Union 36*, 595–600.
Metcalf, W. F. 1960: A note on water movement in the Greenland-Norwegian Sea. *Deep-Sea Res. 7*, 190–200.
Midttun, L. 1985: Formation of heavy bottom water in the Barents Sea. *Deep-Sea Res. 32*, 1233–1241.
Mohn, H. 1887: Nordhavets dybder, temperatur og strømninger. *Den Norske Nordhavsekspedisjon 1876–1878 II.*
Mosby, H. 1959: Deep Water in the Norwegian Sea. *Geofysiske publikasjoner 21.* 62 pp.
Mosby, H. 1961: Recording the formation of bottom water in the Norwegian Sea. Pp. 289–296 in *Proceedings of the symposium on mathematical-hydrodynamical methods of physical oceanography. Inst. Meereskunde.* University of Hamburg. 420 pp.
Nansen, F. 1902: Oceanography of the North Polar Basin. *The Norwegian North Polar Expedition 1893–96. Scientific Results 3(9).* 427 pp.
Nansen, F. 1906: Northern Waters. Captain Roald Amundsen's oceanographic observations in the Arctic Seas in 1901. *Videnskabs-Selskabets Skrifter I. Matematisk-Naturvidenskabelig klasse 1(3).* 145 pp.
Nansen, F. 1915: Spitsbergen Waters. *Videnskabs-Selskabets Skrifter I. Matematisk-Naturvidenskabelig klasse 2.* 132 pp.
Omstedt, A. 1985: *On cooling and initial ice formation in the upper layers of the ocean.* Ph.D. Thesis, Univ. of Gothenburg.
Palfrey, K. M. 1967: *Physical oceanography of the northern part of the Greenland Sea in the summer of 1964.* Master Thesis, Univ. of Washington. 63 pp.
Perkin, R. G. & Lewis, E. L. 1984: Mixing in the West Spitsbergen Current. *J. Phys. Oceanogr. 14(8)*, 1315–1325.
Rudels, B. 1986: On the mass balance of the Polar Ocean, with special emphasis on the Fram Strait. Submitted to *Norsk Polarinstitutt Skrifter.*
Rudels, B. & Anderson, L. 1982: Observations of the mass heat and salt exchange through the Fram Strait. *Report No. 42, Oceanografiska Inst., Univ. of Gothenburg.* 17 pp.
Schumacher, J. D., Aagaard, K., Pease, C. H. & Tripp, R. B. 1983: Effects of a shelf polynya on the flow and water properties in the northern Bering Sea. *J. of Geophys. Res. 88*, 2723–2732.
Scorer, R. S. 1978: *Environmental aerodynamics.* Ellis Horwood, Chichester. 488 pp.
Smith, P. C. 1975: A stream-tube model for the bottom currents in the ocean. *Deep-Sea Res. 22*, 853–875.
Stommel, H. 1972: Deep winter-time convection in the western Mediterranean Sea. Pp. 207–218 in Gordon, A. (ed.): *Studies in Physical Oceanography. A tribute to George Wüst on his 80th birthday, vol. 2.* Gordon & Breach.
Swift, J. H. & Aagaard, K. 1981: Seasonal transitions and water mass formation in the Iceland and Greenland seas. *Deep-Sea Res. 28A(10)*, 1107–1129.
Swift, J. H., Takahashi, T. & Livingston, H. D. 1983: The contribution of the Greenland and the Barents seas to the deep water of the Arctic Ocean. *J. Geoph. Res. 88*, 5981–5986.
Turner, J. S. 1973: *Buoyancy effects in fluids.* Cambridge Univ. Press, Cambridge. 367 pp.
Wakatsuchi, M. 1983: Brine exclusion process from growing sea ice. *Contributions from the Institute of Low Temperature Science, Hokkaido Univ., Sapporo*, 29–65.
Weiss, R. F., Östlund, M. G. & Craig, H. 1979: Geochemical studies of the Weddell Sea. *Deep-Sea Res. 26*, 1093–1120.